CONFLUENT

Volume weighted probabilistic methods for nitinol lifetime prediction

Craig Bonsignore

Karthikeyan Senthilnathan

Ali Shamimi

Confluent Medical Technologies | Fremont California

> **Introduction**

Volumetric FEA methods

Sub-µm x-ray computed tomography

Monte-Carlo risk assessment

Resources

Motivation

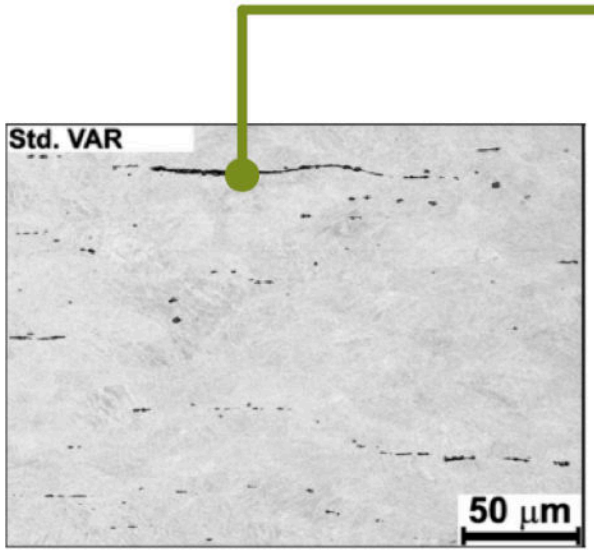

volumetric distribution of material impurities

volumetric distribution of critical regions

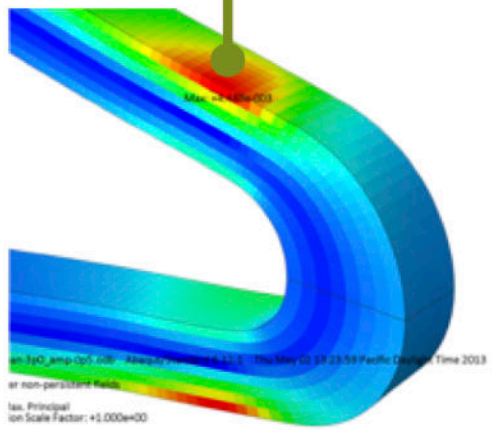

volumetric hazard probability

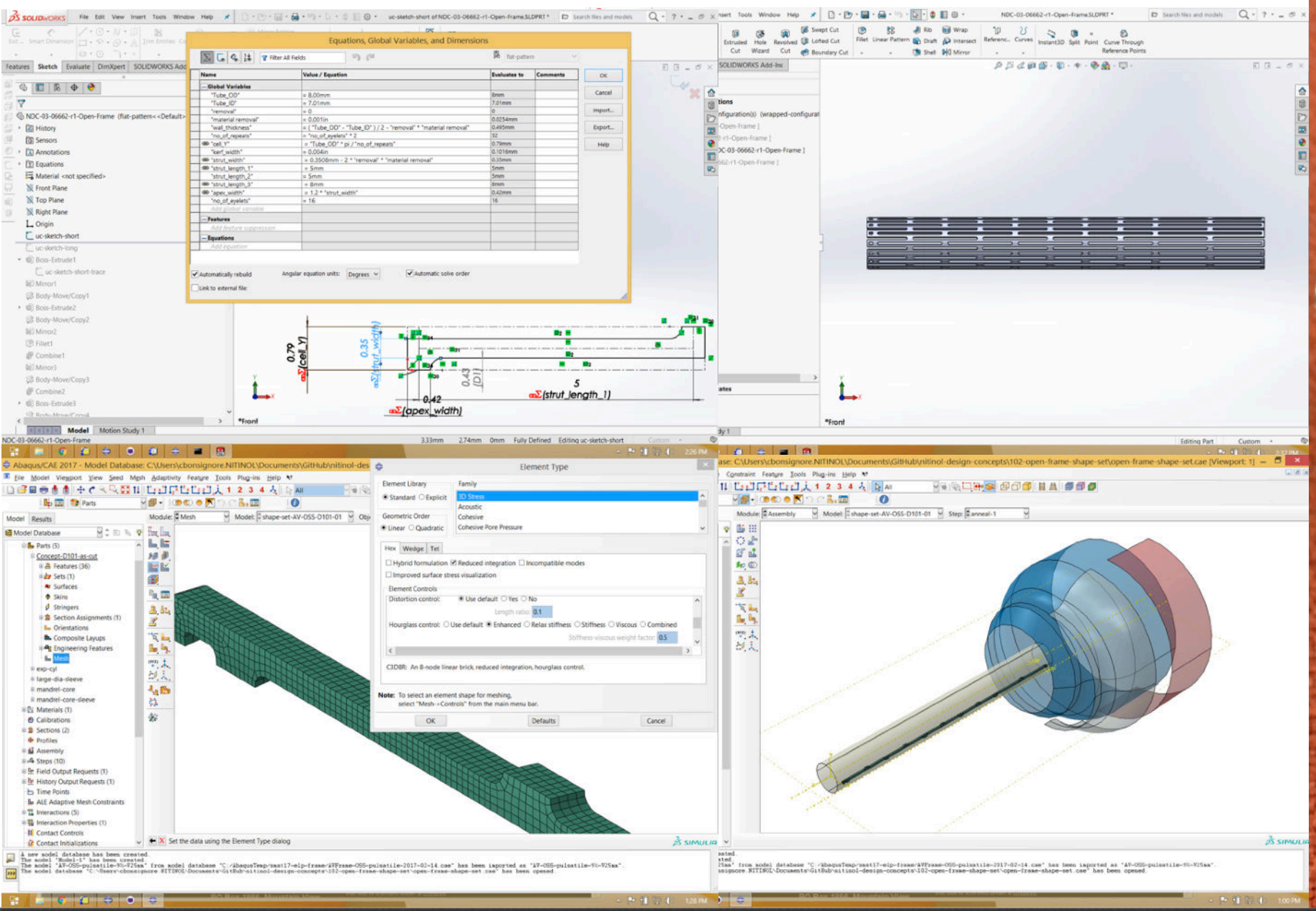

SMST2017

SHAPE MEMORY AND SUPERELASTIC TECHNOLOGIES CONFERENCE AND EXPOSITION

cyclic fatigue condition

9% cyclic change in diameter

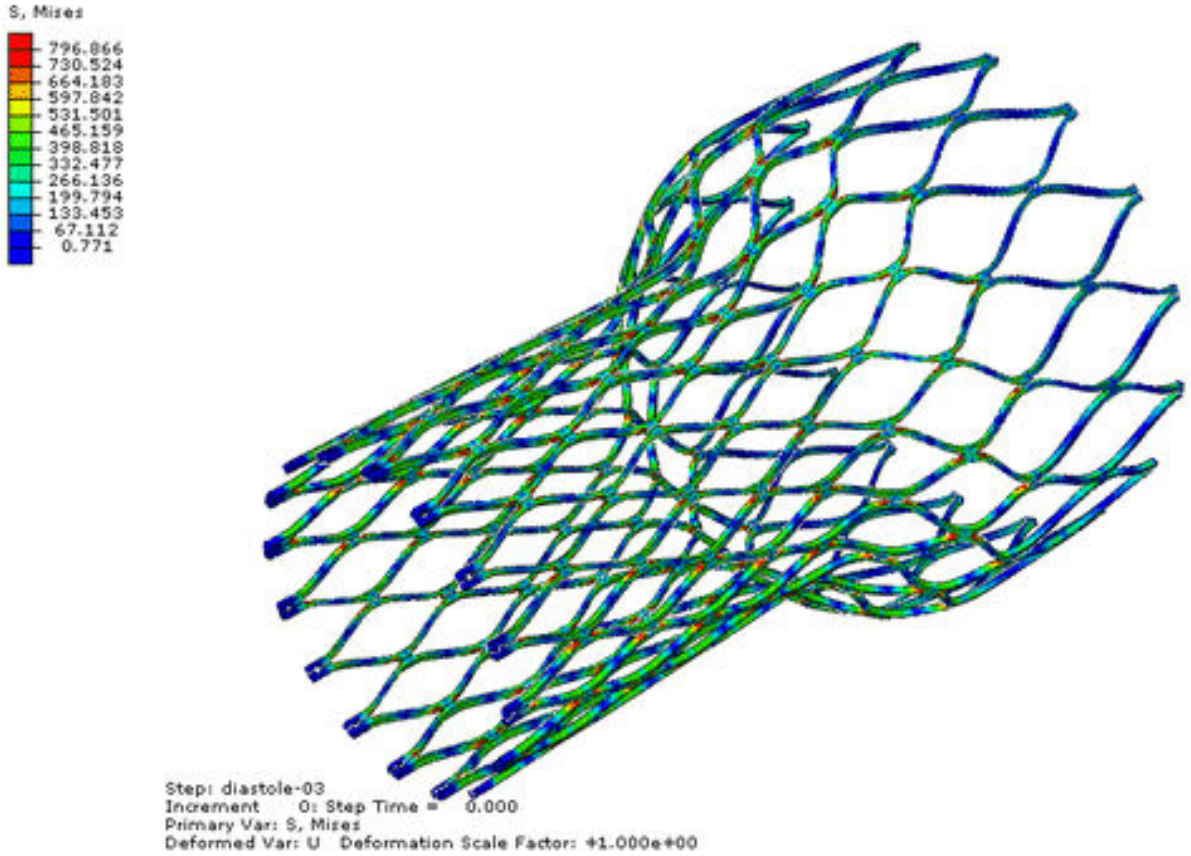

typical point cloud

9% cyclic change in diameter

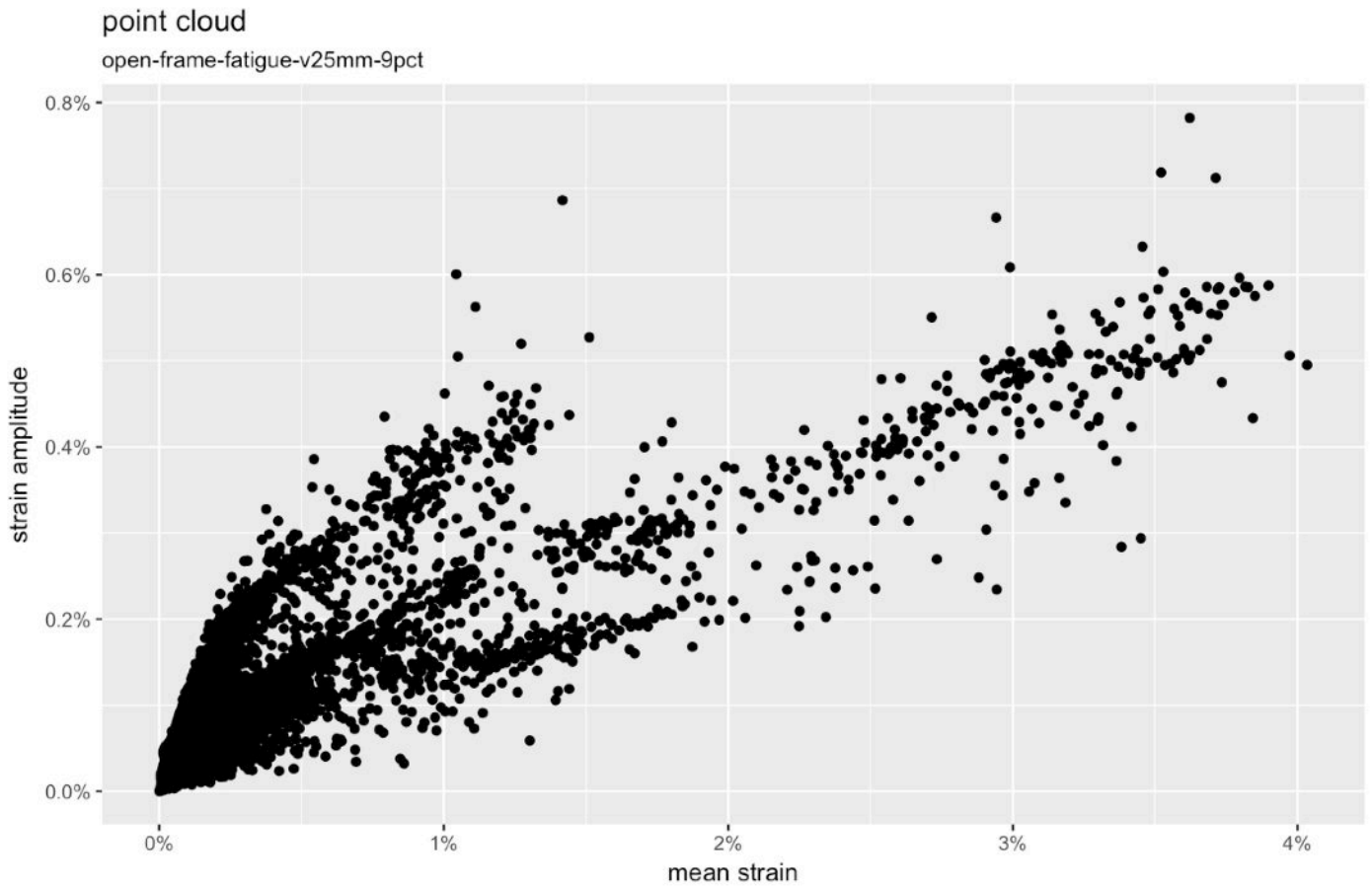

critical volumes

a small proportion of the volume exceeds a critical limit of strain amplitude.

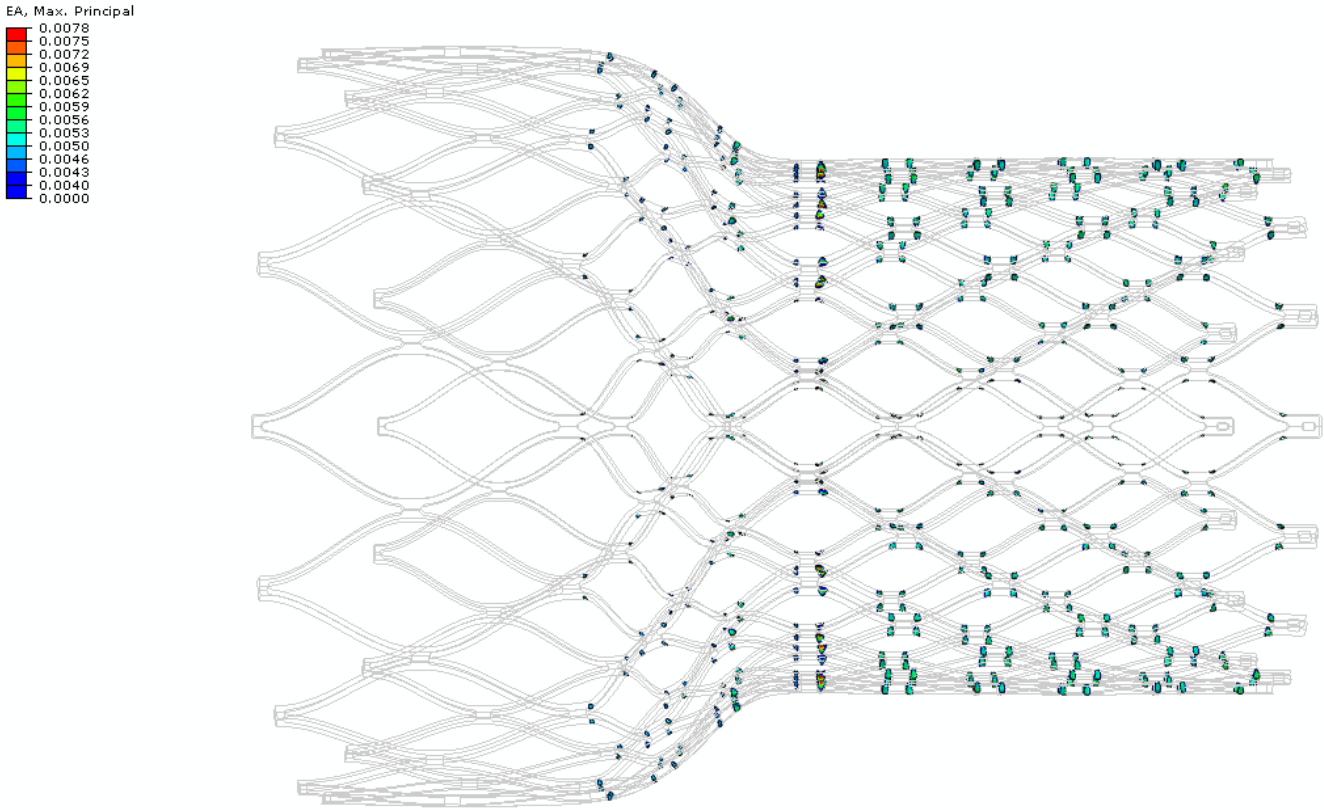

Introduction

> **Volumetric FEA methods**

Sub-µm x-ray computed tomography

Monte-Carlo risk assessment

Resources

Tools to extract volume data and more

- integration point volume
- strain, stress at crimping step (pre-strain)
- hydrostatic pressure (tension vs. compression)
- volume fraction of martensite
- mean stress/strain
- stress/strain amplitude
- stress and strain components

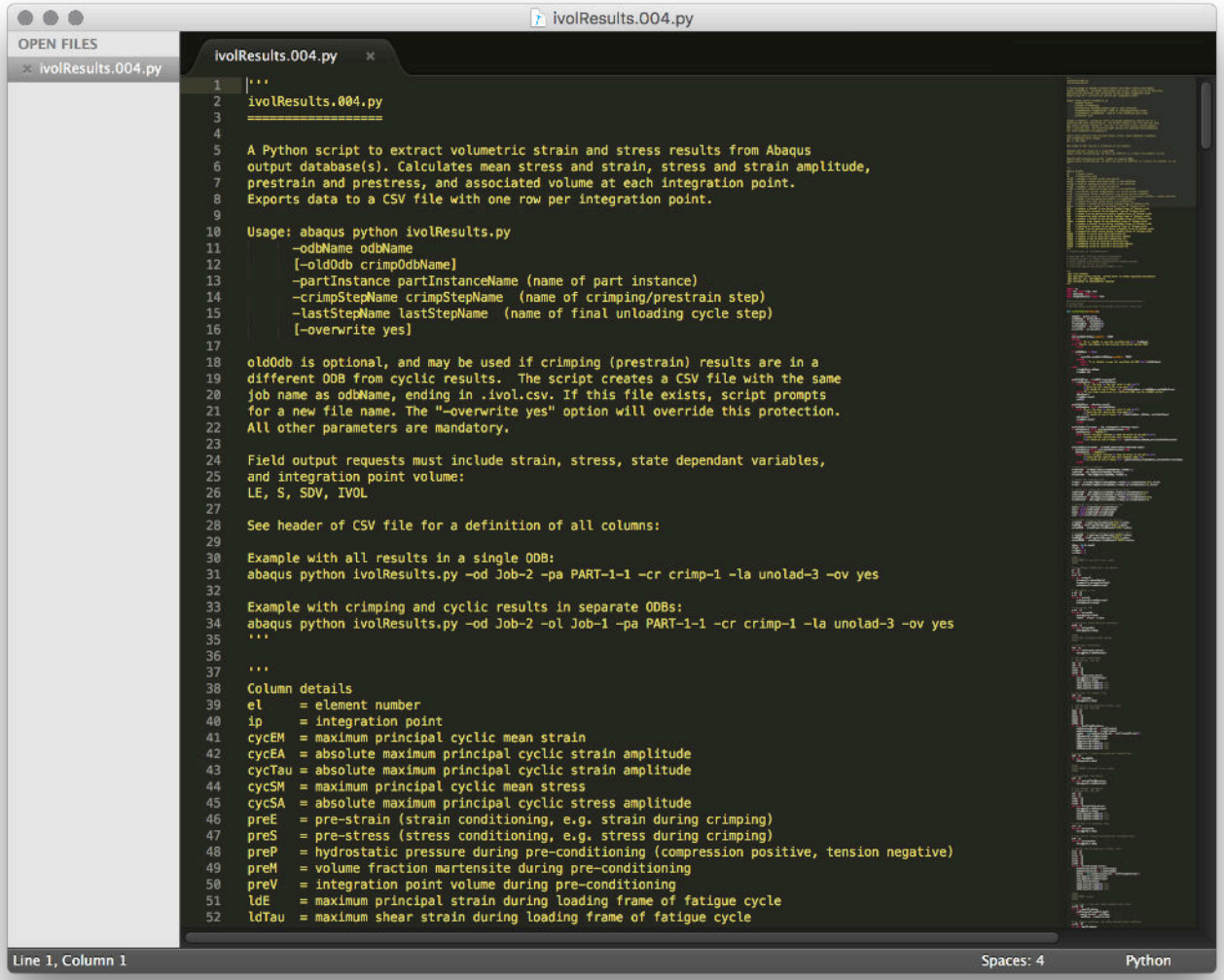

Typical point cloud

strain amplitude vs. mean strain

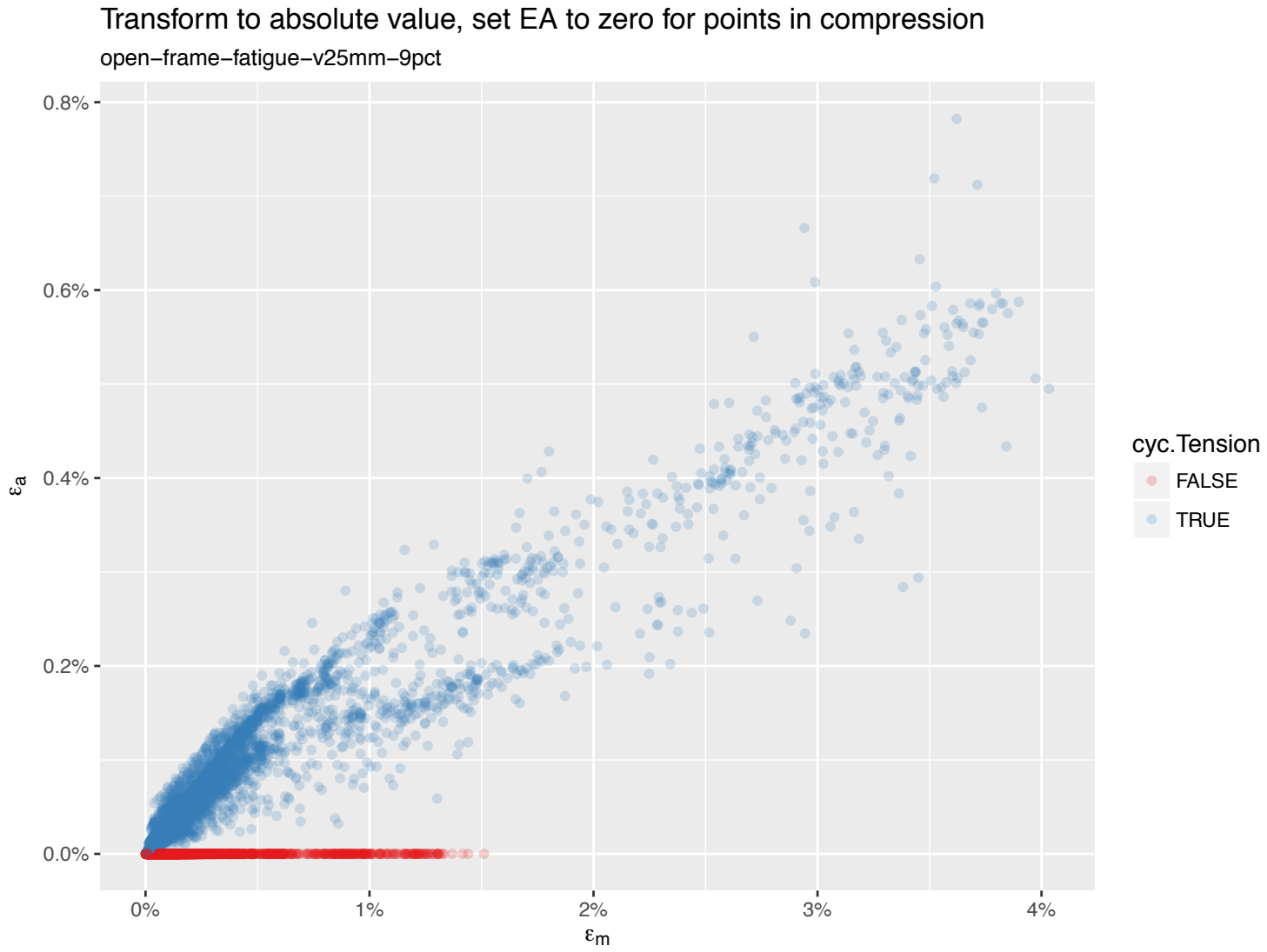

SWT point cloud

Smith-Watson-Topper

(maximum stress)·(strain amplitude)

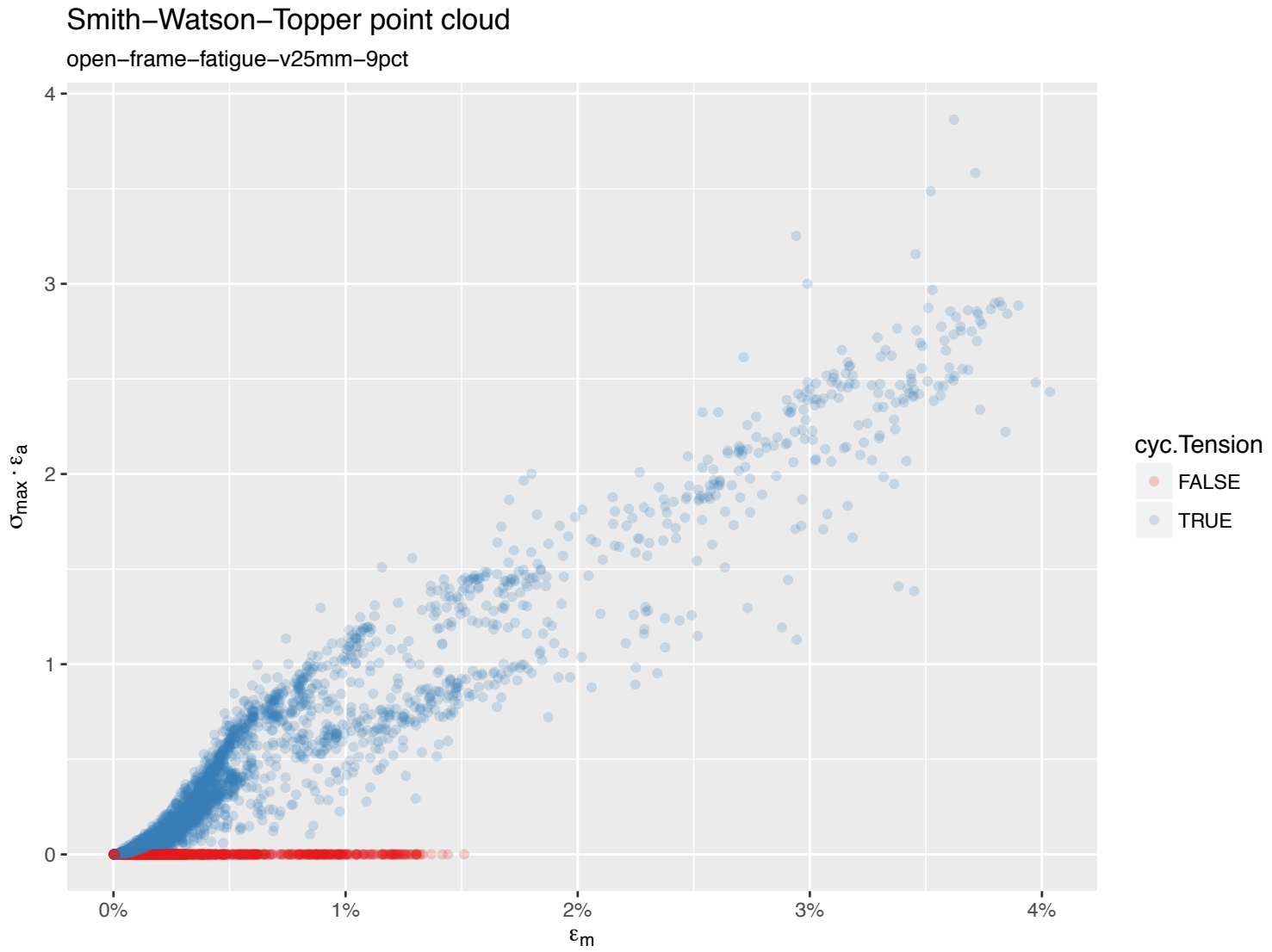

Phase map

During the fatigue cycle, elements may:

- Remain austenite throughout
- Remain martensite throughout
- Alternate A/M during cycle

Point cloud highlighting phase of each element during cycle

open–frame–fatigue–v25mm–9pct

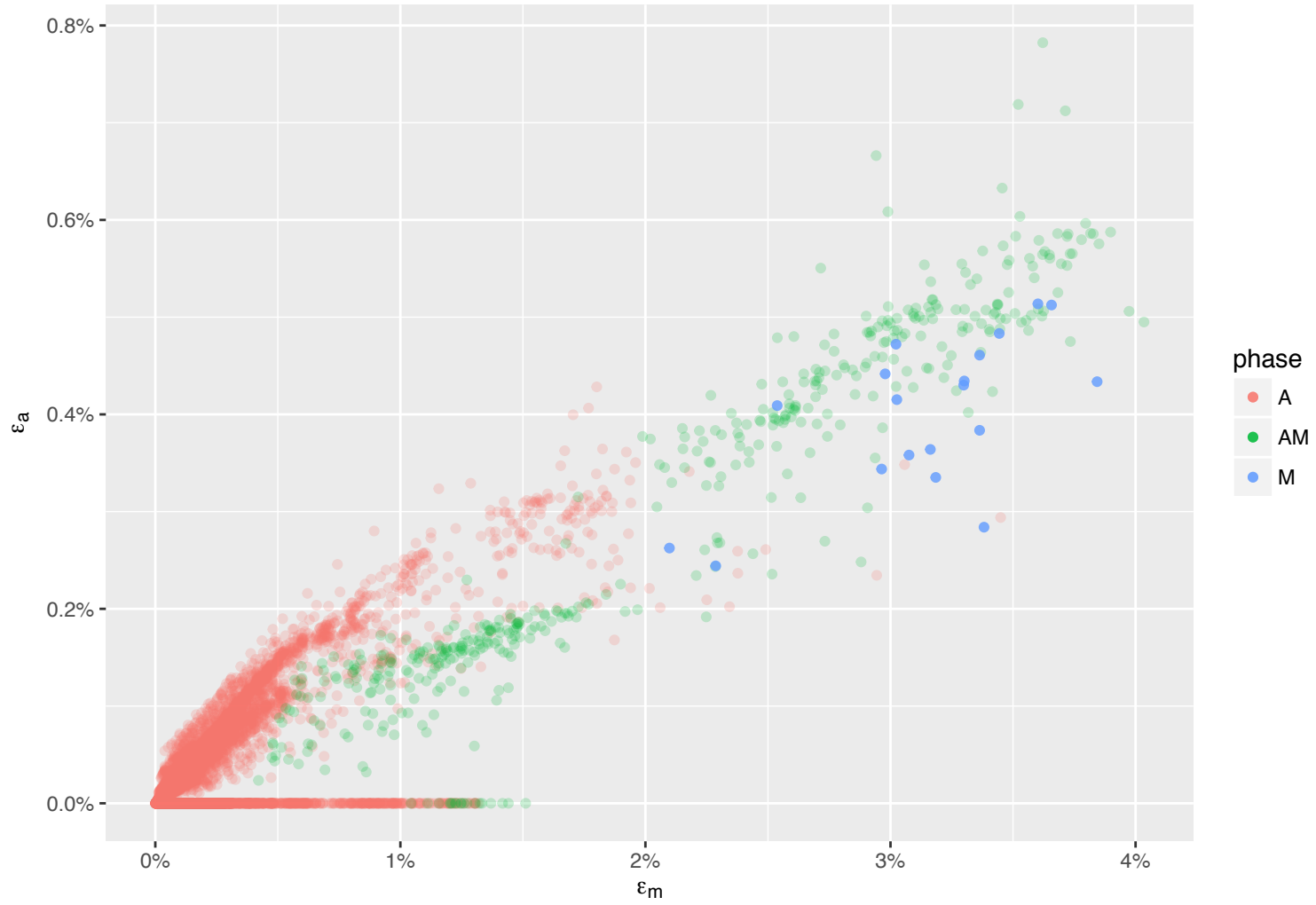

Volumetric histogram

Measure the total volume of material in each phase, according to strain amplitude (or SWT, or any other criterion)

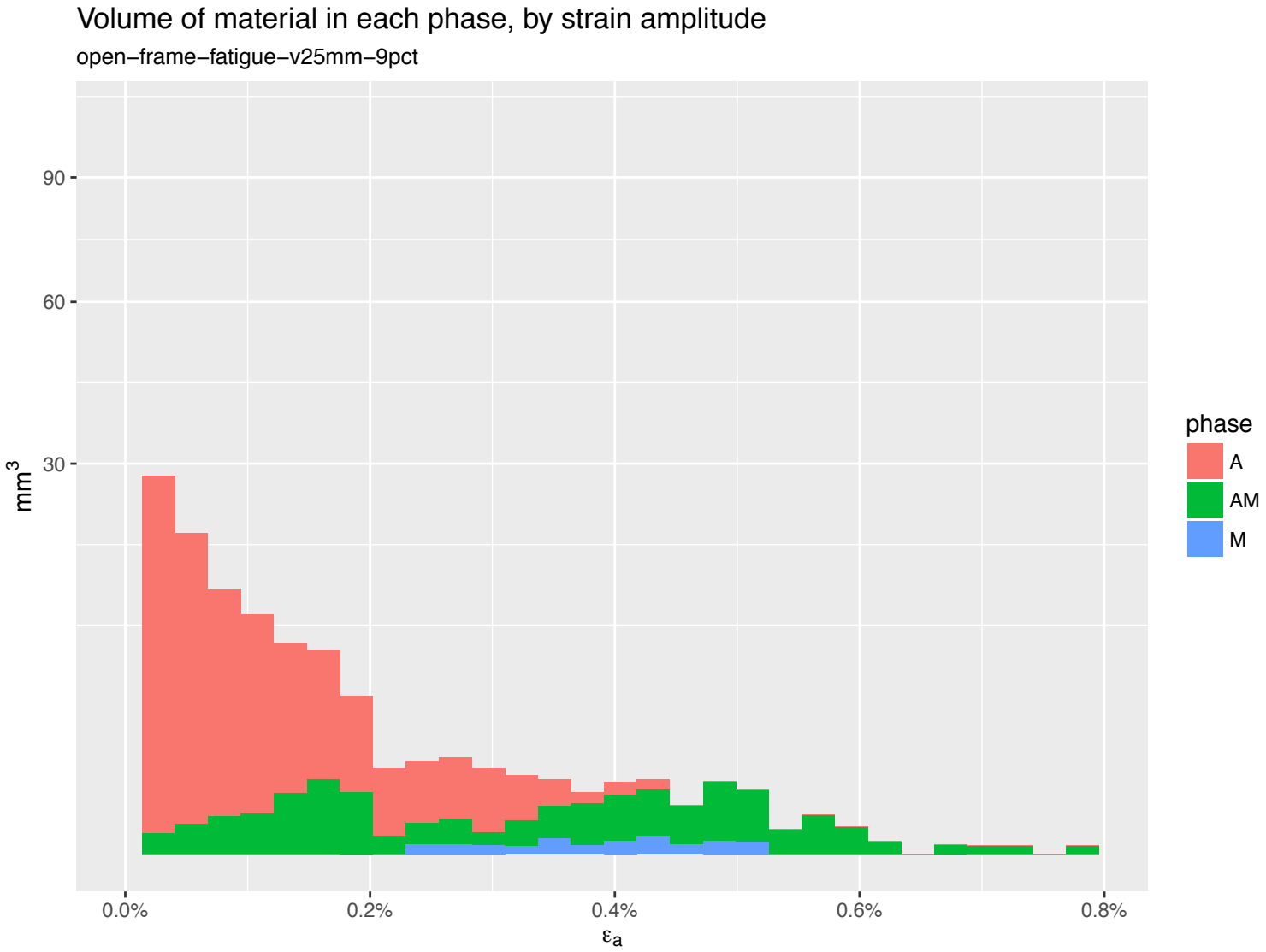

Introduction
Volumetric FEA methods
> **Sub-µm x-ray computed tomography**
Monte-Carlo risk assessment
Resources

Standard VAR (SE508)

264.46x198.35 µm (1280x960); 8-bit; 1.2MB

High Purity VAR (SE508-ELI)

264.46x198.35 µm (1280x960); 8-bit; 1.2MB

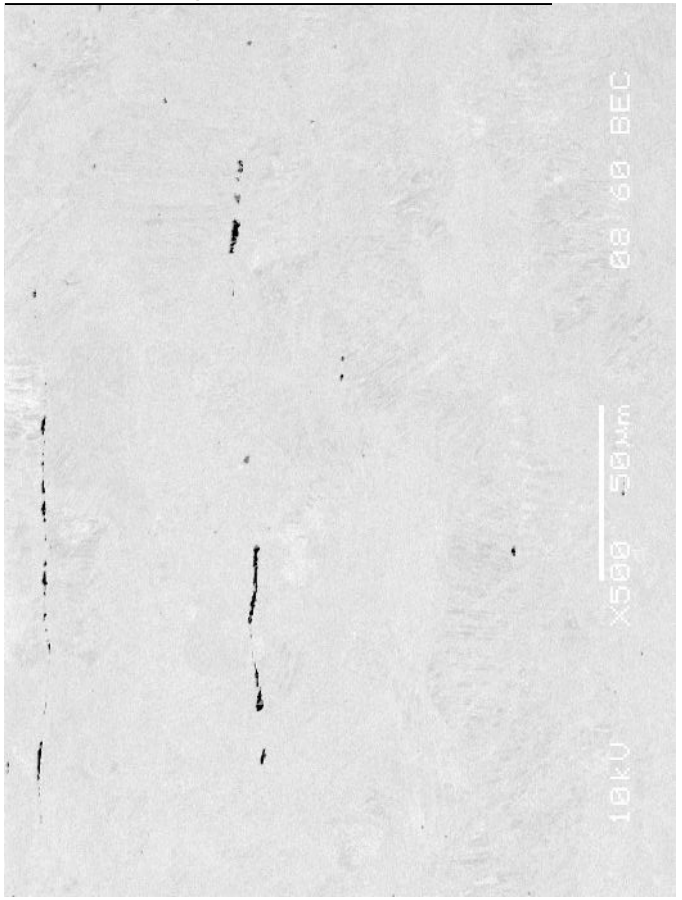

Approximation of inclusion volumetric probability

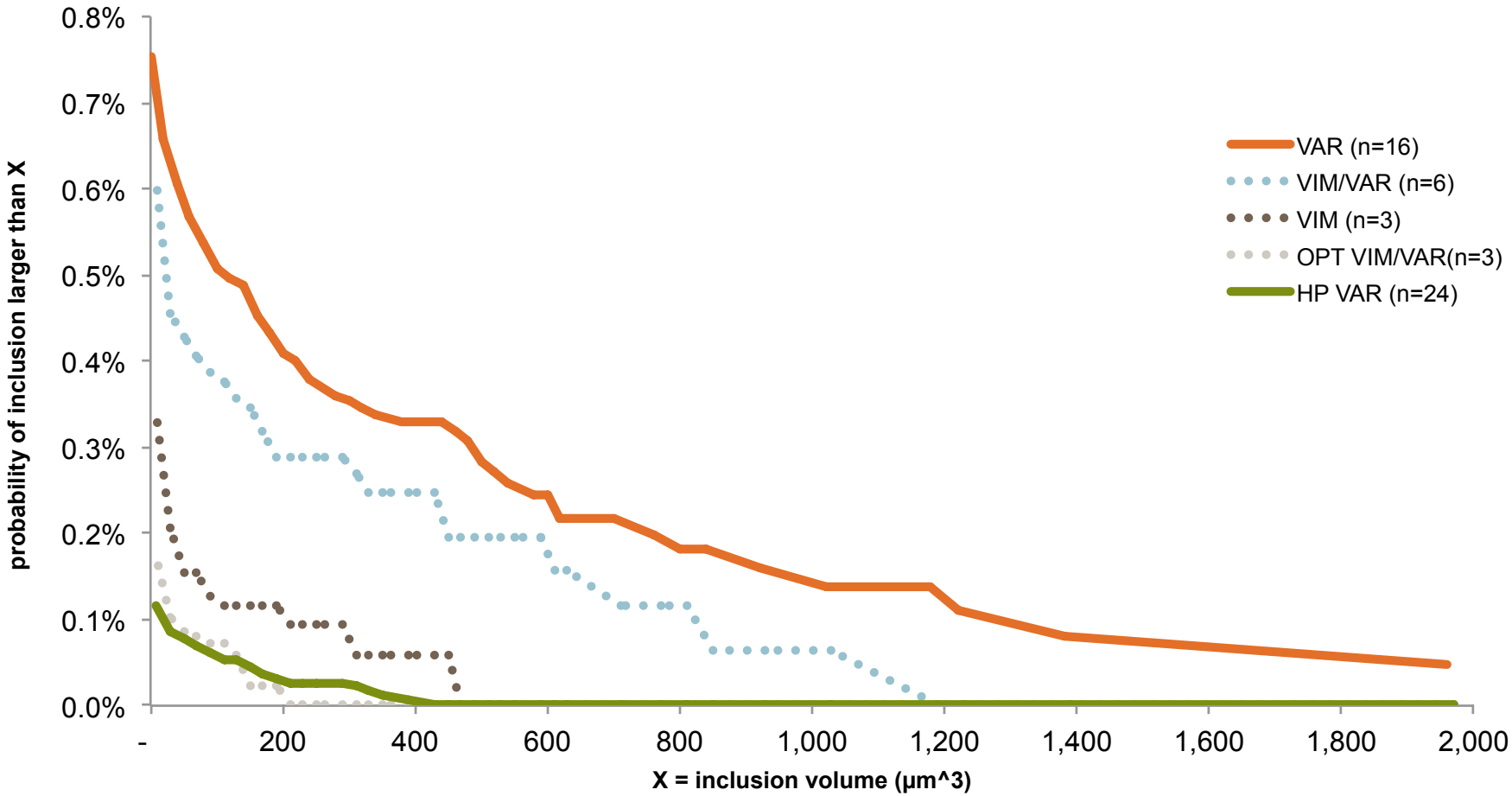

Durability performance benefit of high purity material

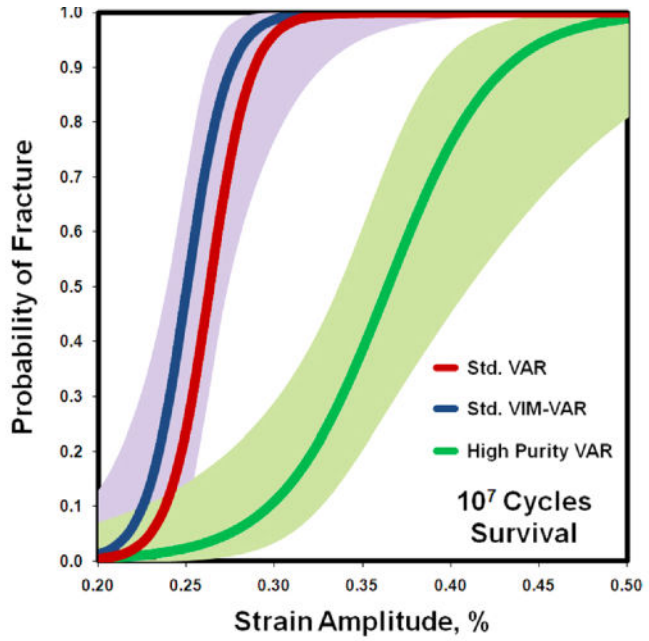

Fig. 8 – Probability of Nitinol wire fracture versus strain amplitude plots with the curve fit line shown bracketed by the 95th percentile upper and lower confidence interval bands.

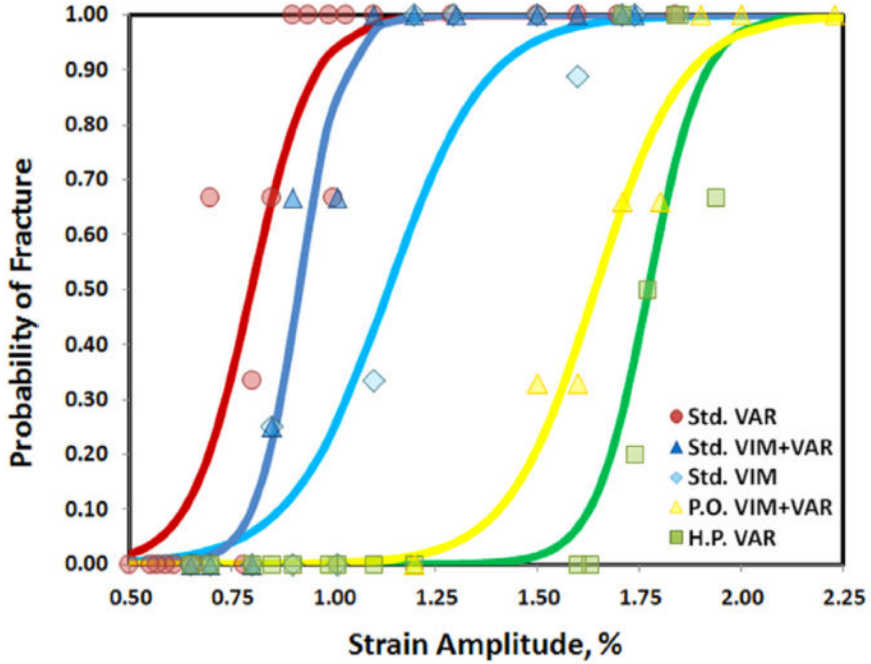

Fig. 9 – Probability of Nitinol diamond fracture at 10^7 cycles versus strain amplitude plots with a logit sigmoidal curve fit line for each data set.

Robertson, S. W. et al. A statistical approach to understand the role of inclusions on the fatigue resistance of superelastic Nitinol wire and tubing. J. Mech. Behav. Biomed. Mater. 51, 119–131 (2015).

X-ray computed tomography (XCT) test specimens

8.00x7.01 superelastic nitinol tubing
0.5mm x 0.5mm x 50mm laser cut “matchstick” samples

scan01: SE508
scan02: SE508ELI
scan03: SE508ELI

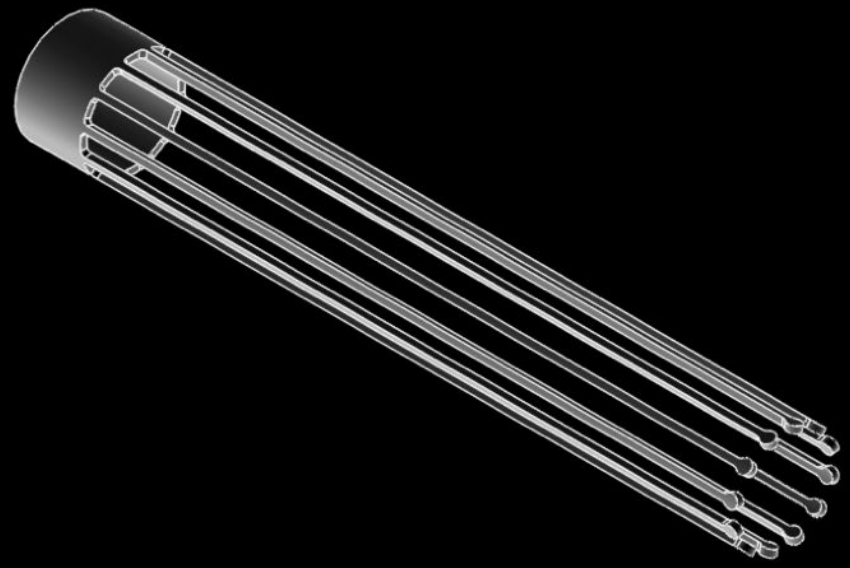

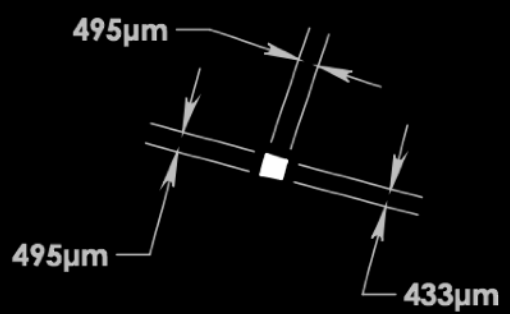

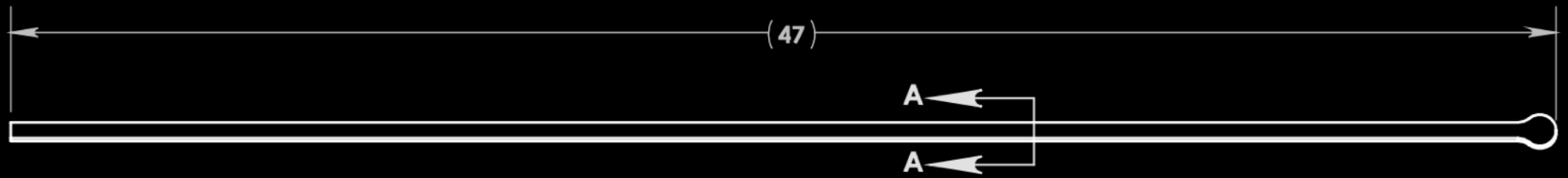

XCT scan output: 1,994 16-bit images (0.50μm^3 voxel)

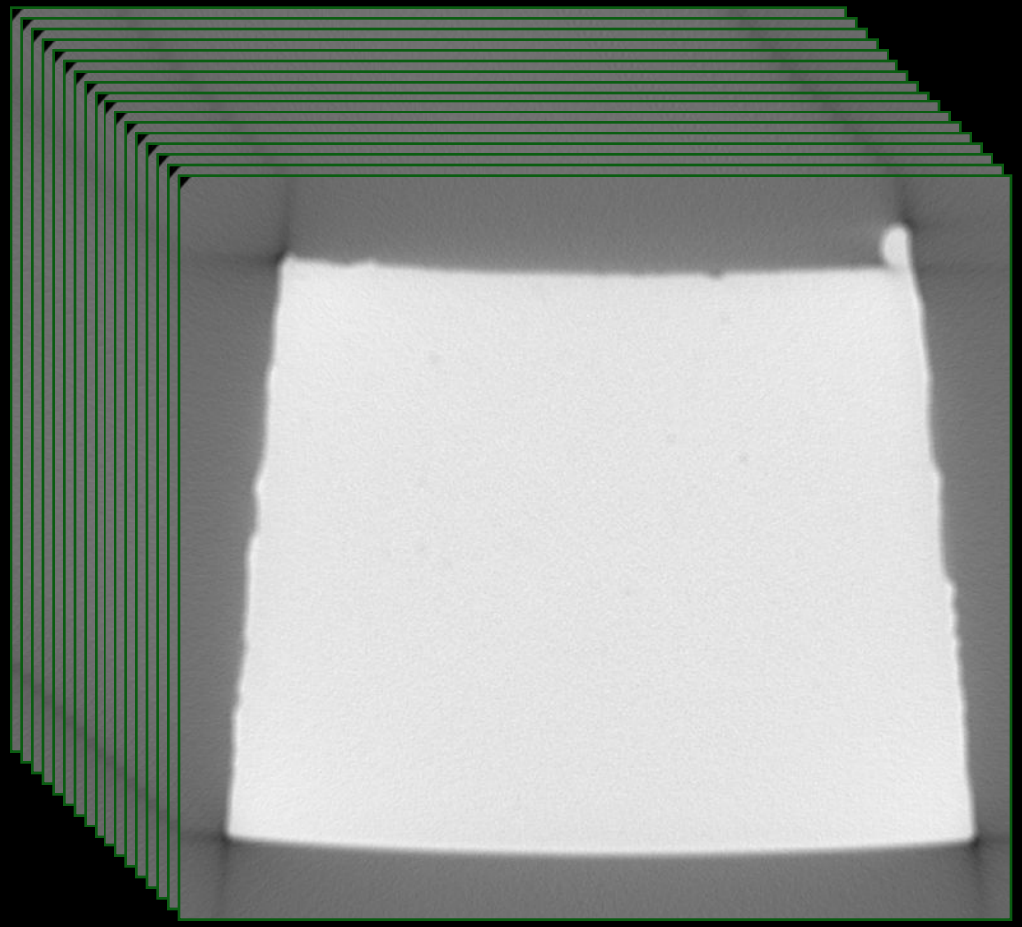

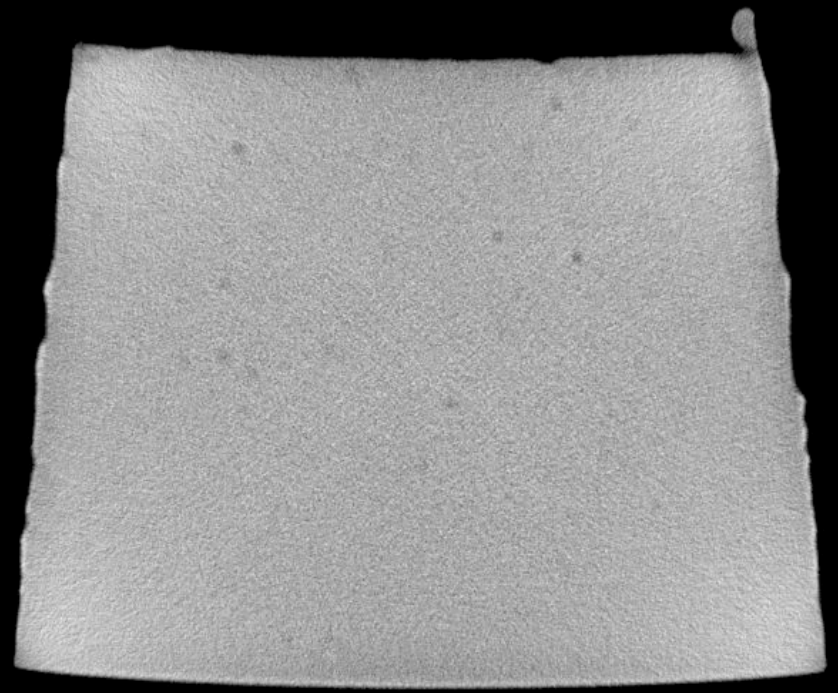

Image segmentation by machine learning

Fiji [1] is just ImageJ [2]

Trainable Weka Segmentation [3]

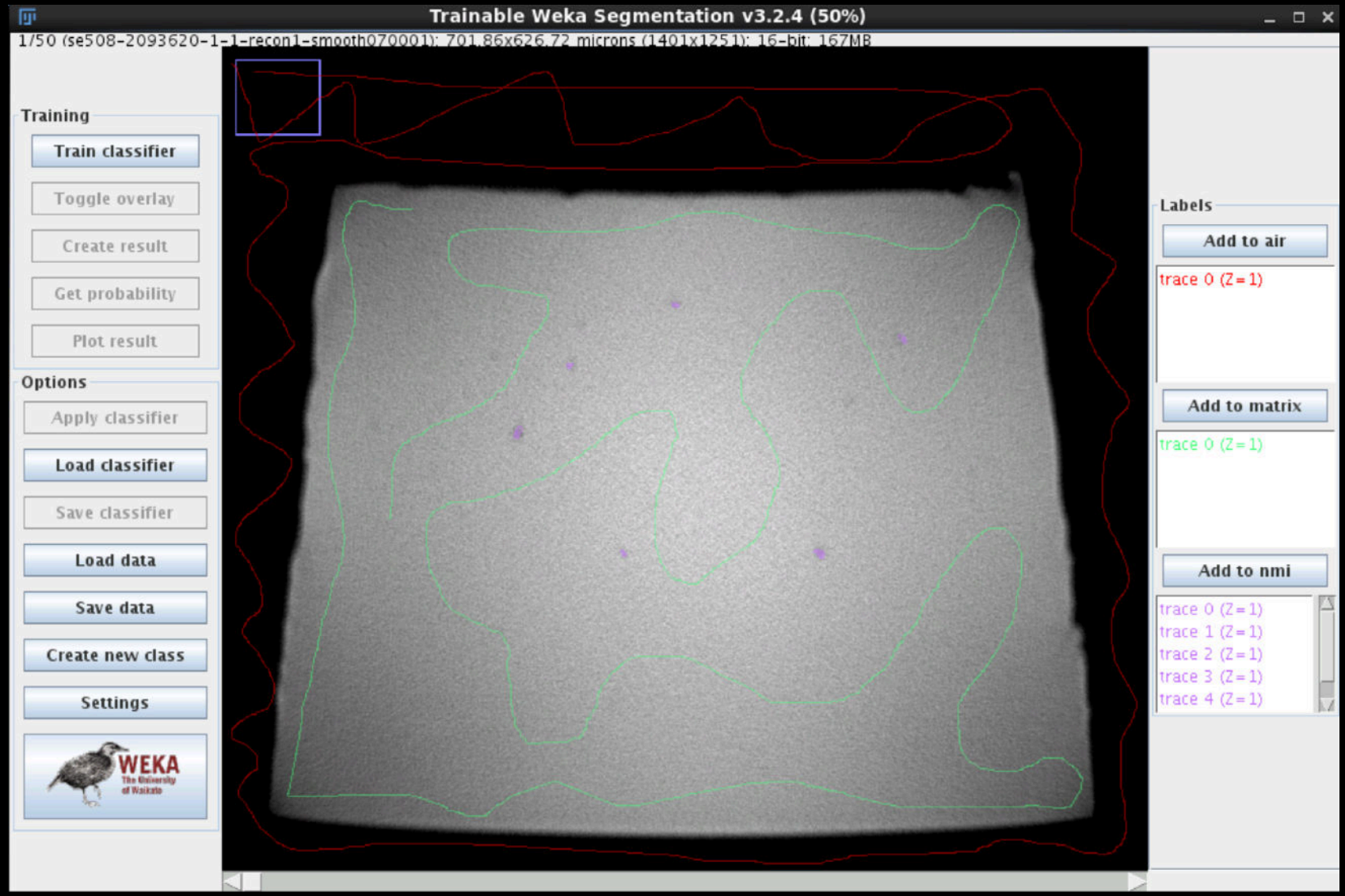

[1] J. Schindelin, I. Arganda-Carreras, E. Frise, V. Kaynig, M. Longair, T. Pietzsch, S. Preibisch, C. Rueden, S. Saalfeld, B. Schmid, J.-Y. Tinevez, D.J. White, V. Hartenstein, K. Eliceiri, P. Tomancak, A. Cardona, Fiji: an open-source platform for biological-image analysis., Nat. Methods. 9 (2012) 676–82. doi:10.1038/nmeth.2019.

[2] M.D. Abràmoff, P.J. Magalhães, S.J. Ram, Image processing with imageJ, Biophotonics Int. 11 (2004) 36–41. doi:10.1117/1.3589100.

Voxel Classification

Train classifier to identify probability of each voxel as:

- matrix
- nmi (inclusion/void)
- air
- edge

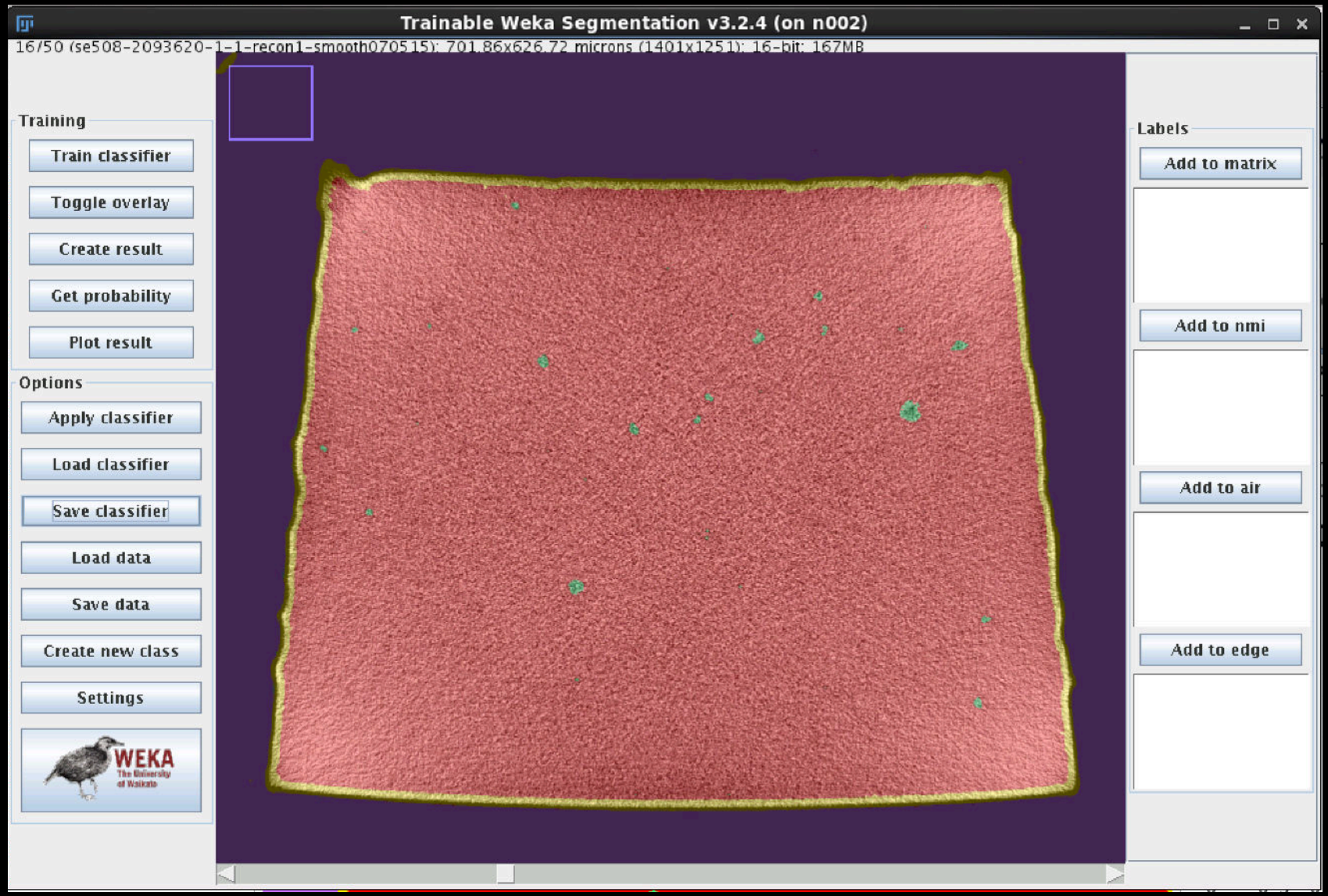

[3] I. Arganda-Carreras, V. Kaynig, J. Schindelin, A. Cardona, H.S. Seung, Trainable Weka Segmentation: A Machine Learning Tool for Microscopy Image Segmentation, Neurosci. 2014 Short Course 2 - Adv. Brain-Scale, Autom. Anat. Tech. Neuronal Reconstr. Tract Tracing, Atlasing. (2014) 73--80.

SE508 maximum intensity projection of inclusion probability

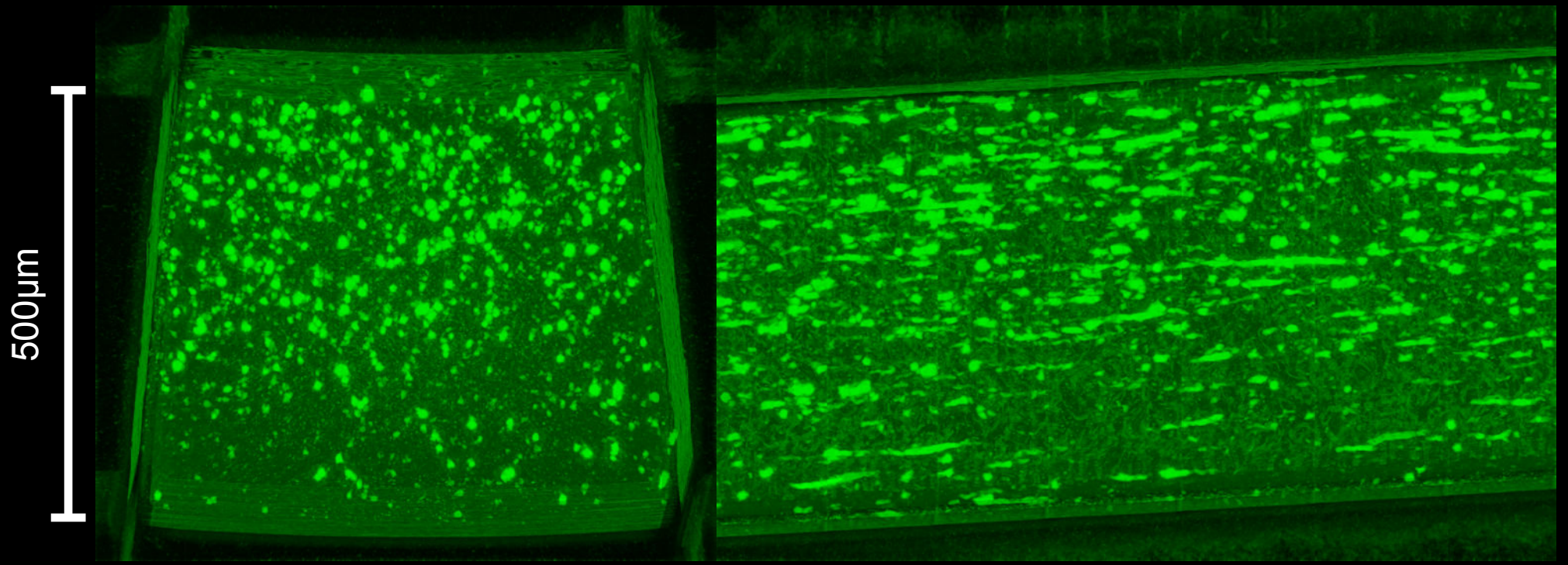

visualization superimposes all inclusions through 500µm thickness

SE508-ELI maximum intensity projection of inclusion probability

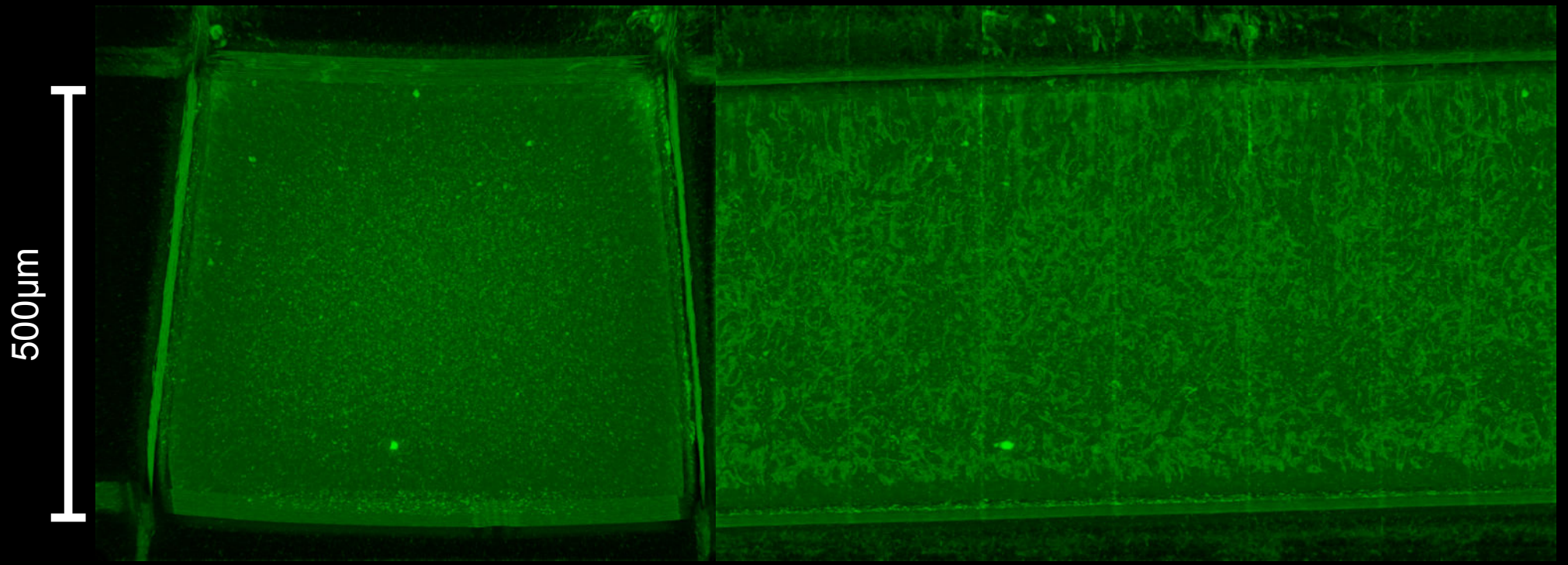

visualization superimposes all inclusions through 500µm thickness

SE508 inclusion segmentation colored by volume

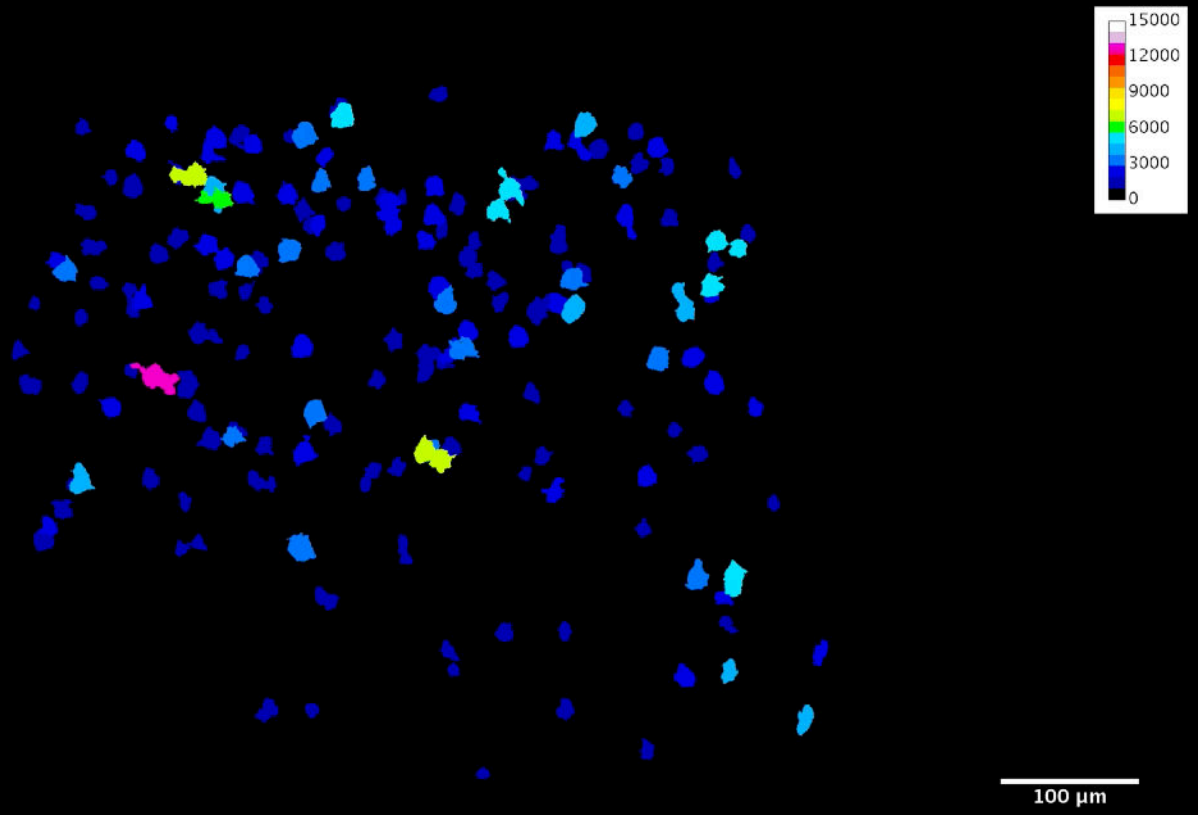

[1] D. Legland, I. Arganda-Carreras, P. Andrey, MorphoLibJ: integrated library and plugins for mathematical morphology with ImageJ, Bioinformatics. (2016) btw413. doi:10.1093/bioinformatics/btw413.

SE508-ELI inclusion segmentation colored by volume

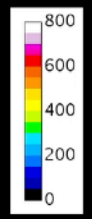

[1] D. Legland, I. Arganda-Carreras, P. Andrey, MorphoLibJ: integrated library and plugins for mathematical morphology with ImageJ, Bioinformatics. (2016) btw413. doi:10.1093/bioinformatics/btw413.

Volumetric distribution of inclusions

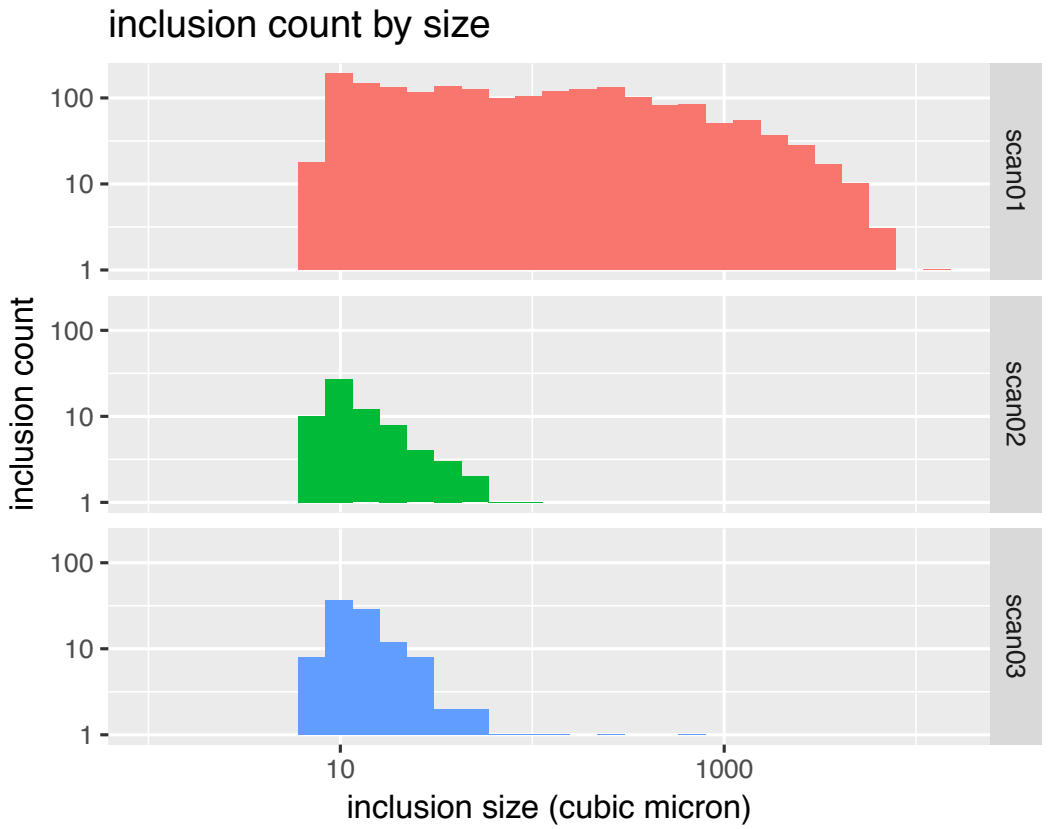

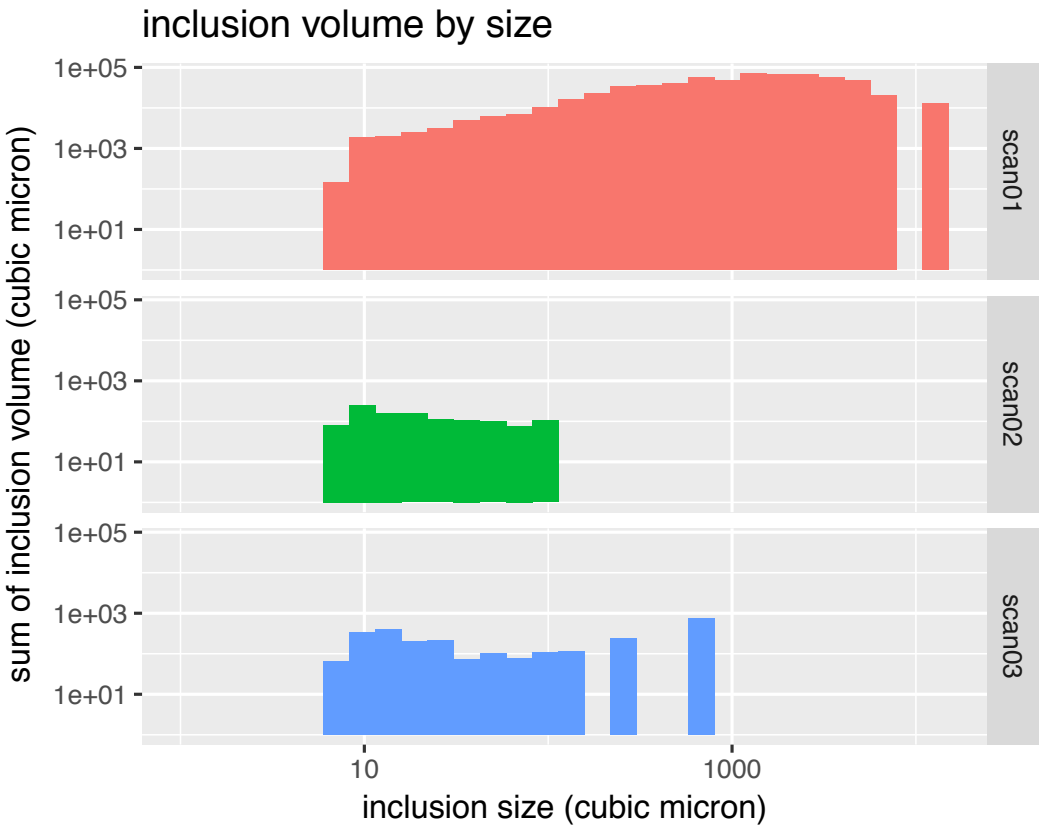

* *note log-log scales*

√Area fit to Extreme Value Distribution per Urbano[1]

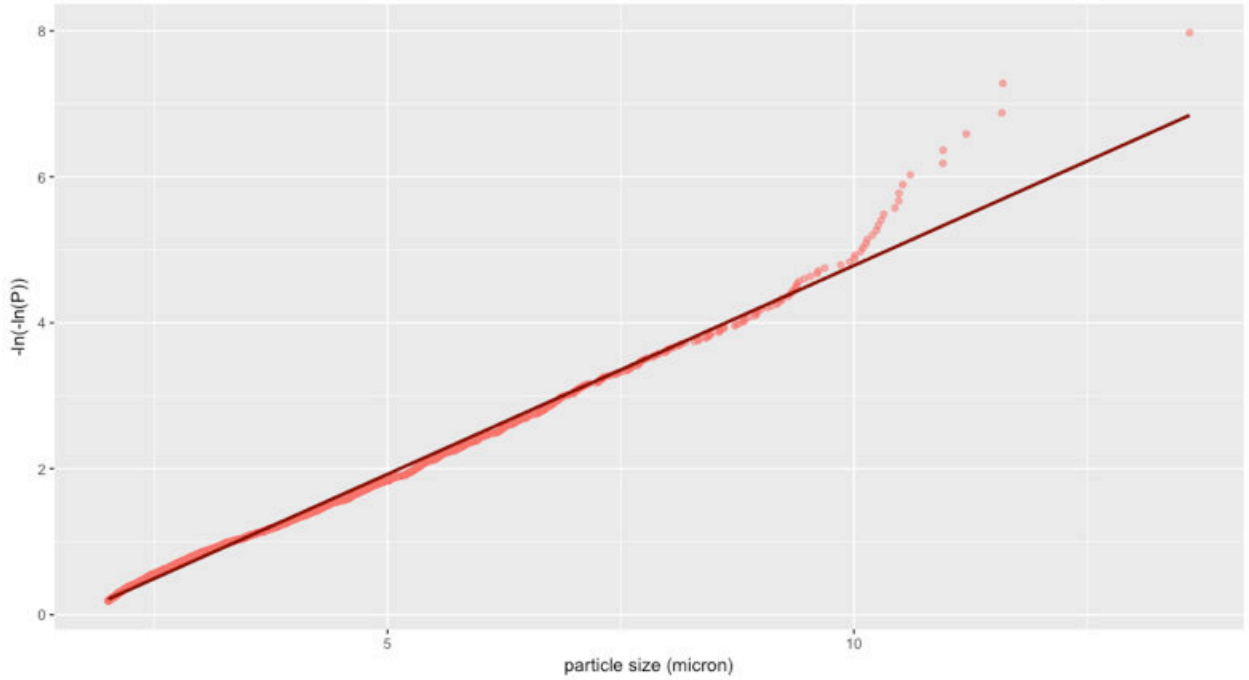

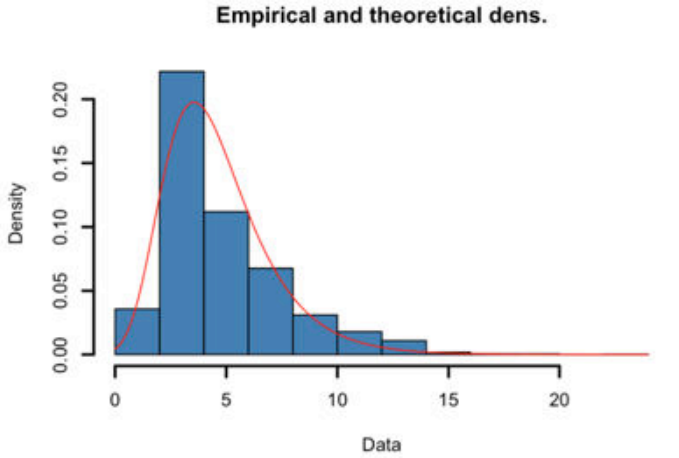

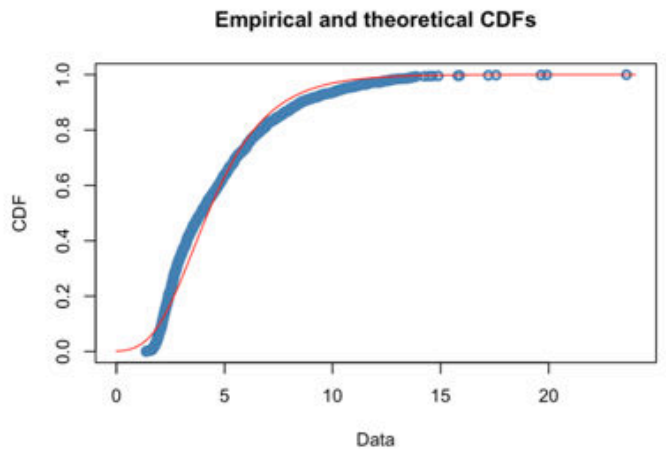

[1] M.F. Urbano, A. Cadelli, F. Sczerzenie, P. Luccarelli, S. Beretta, A. Coda, Inclusions Size-based Fatigue Life Prediction Model of NiTi Alloy for Biomedical Applications, Shape Mem. Superelasticity. 1 (2015) 1–12.

Inclusion density, Gumbel location and scaling parameters

SE508 Inclusion Distribution Parameters

plane	cutoff (μm^3)	inclusion density ($1/mm^3$)	Gumbel μ (μm)	Gumbel σ (μm)
xy (transverse)	8	7,475	2.84	1.36
yz (longitudinal)	8	7,475	3.59	1.96
xz (longitudinal)	8	7,475	3.55	1.86

ELI Inclusion Distribution Parameters

plane	cutoff (μm^3)	inclusion density ($1/mm^3$)	Gumbel μ (μm)	Gumbel σ (μm)
xy (transverse)	8	340	1.77	0.40
yz (longitudinal)	8	340	2.06	0.40
xz (longitudinal)	8	340	2.27	0.45

Fingerprint by Mitchell Eva, from the Noun Project

Introduction
Volumetric FEA methods
Sub-µm x-ray computed tomography
> **Monte-Carlo risk assessment**
Resources

Quantile function: *calculate random defects with sizes following the Gumbel distribution for each material*

$$Q(p) = \mu - \sigma \ \ln[-\ln(p)]$$

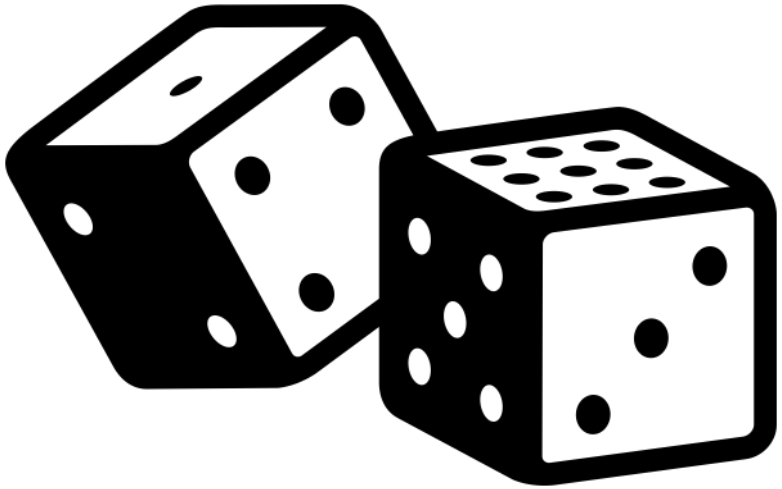

$Q(U)$ has a Gumbel distribution
for random values of U drawn from
a uniform distribution on the interval (0,1)

Dice by b farias, from the Noun Project

“Fortune cloud”: Δσ vs. √area (single run SE508, ELI)

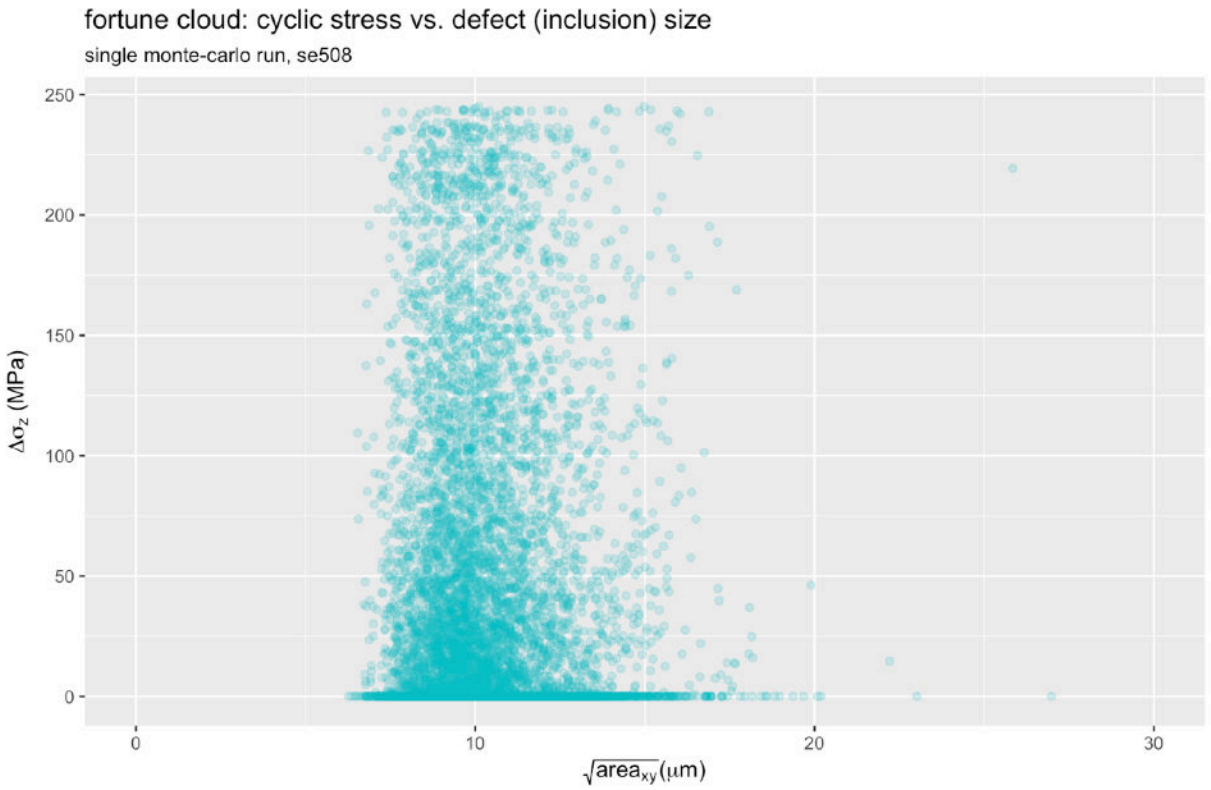

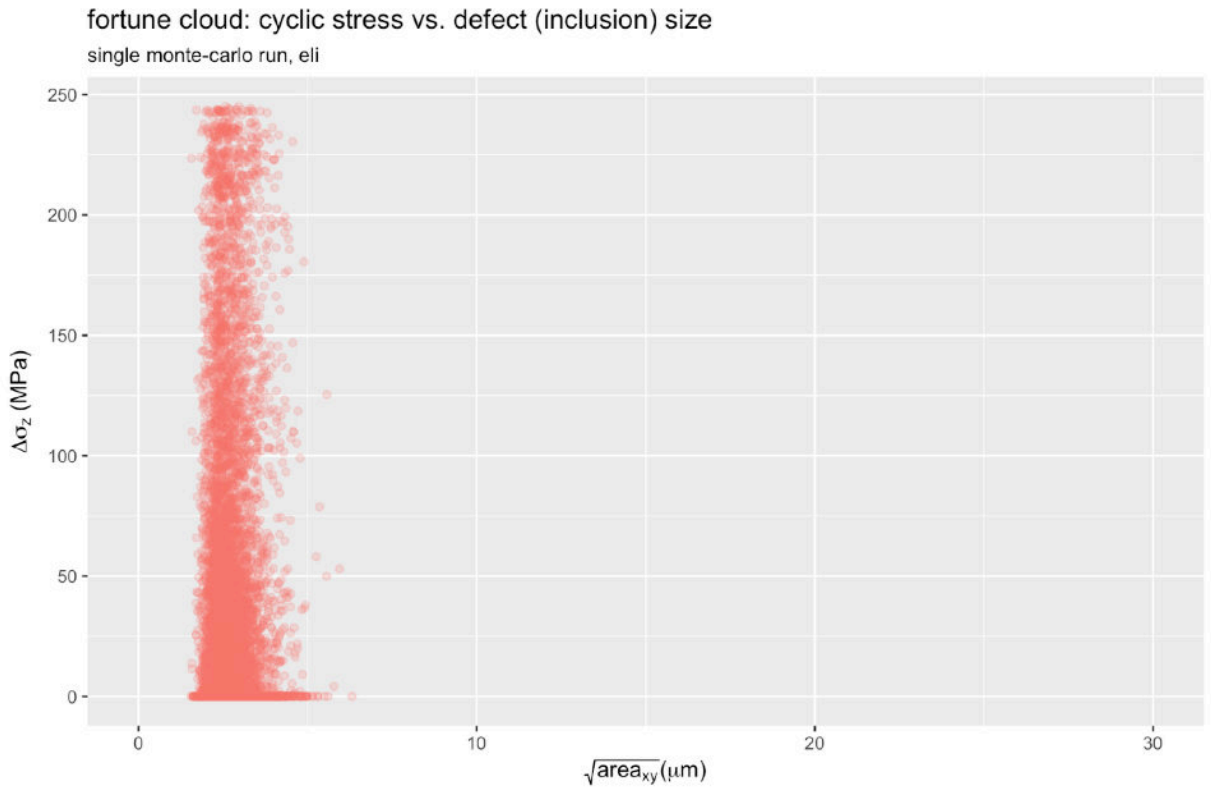

Estimating stress intensity factor K by Murakami's √area

FEA

XCT, Gumbel Parameters

$$K\left(\sigma, \sqrt{area}\right) = 0.65 \cdot \sigma \sqrt{\pi \cdot \sqrt{area}}$$

Figure 7 shows the relationship between the maximum stress intensity factor K_{Imax} and $\sqrt{area}$ for surface cracks (elastic analysis) **(24)(25)**. (See also **(20)(66)**.)

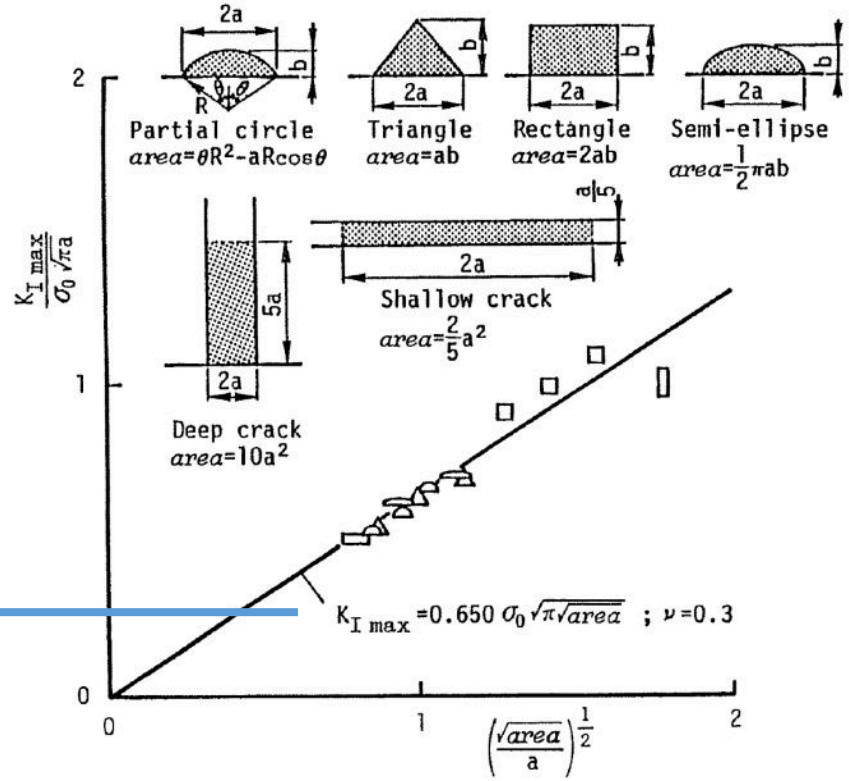

Murakami Y, Endo M (1986) Effect of hardness and crack geometries on ΔK_{th} of small cracks emanating from small defects, In: The Behavior of Short Fatigue Cracks, EGF Pub. 1, pp 275–293

K and ΔK in each plane, at each integration point

$$K_x = 0.65 \cdot \sqrt{\sigma_x \cdot \sqrt{area_{yz}}} \qquad \Delta K_x = 0.65 \cdot \sqrt{\Delta\sigma_x \cdot \sqrt{area_{yz}}}$$

$$K_y = 0.65 \cdot \sqrt{\sigma_y \cdot \sqrt{area_{xz}}} \qquad \Delta K_y = 0.65 \cdot \sqrt{\Delta\sigma_y \cdot \sqrt{area_{xz}}}$$

$$K_z = 0.65 \cdot \sqrt{\sigma_z \cdot \sqrt{area_{xy}}} \qquad \Delta K_z = 0.65 \cdot \sqrt{\Delta\sigma_z \cdot \sqrt{area_{xy}}}$$

“K point cloud” (single run SE508, ELI)

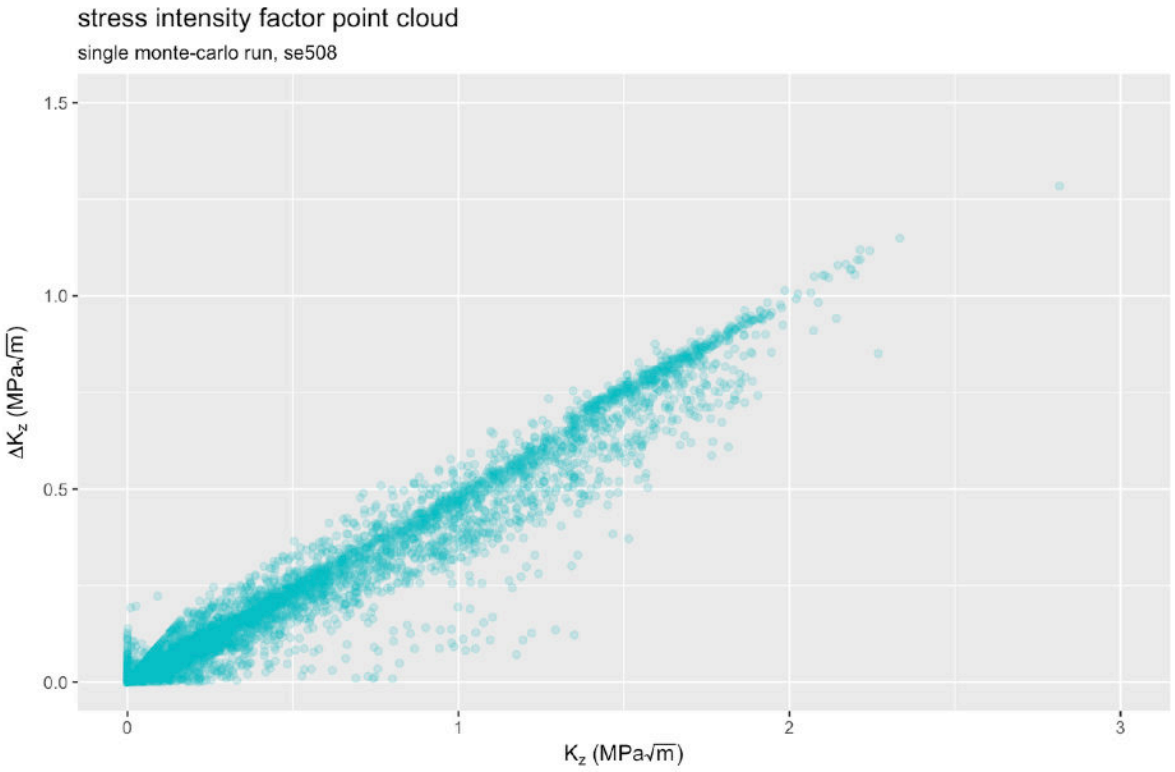

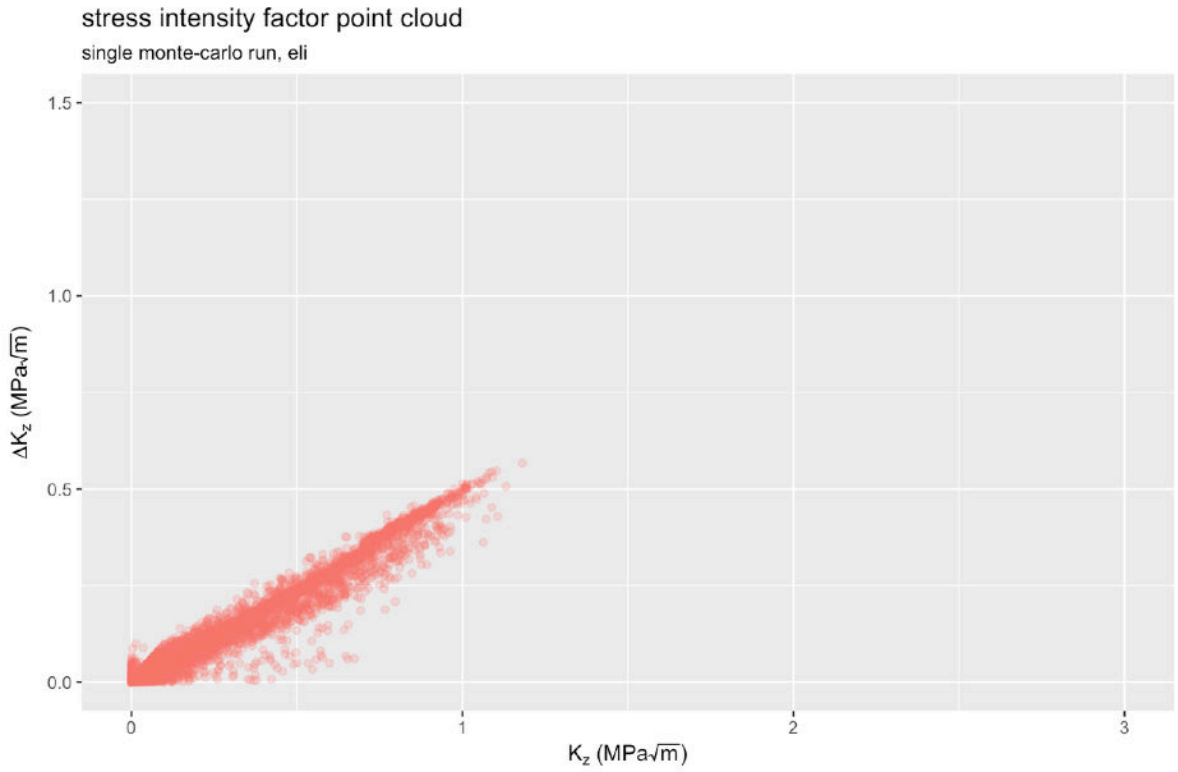

Next: repeat many times, record ΔK_{max} and K

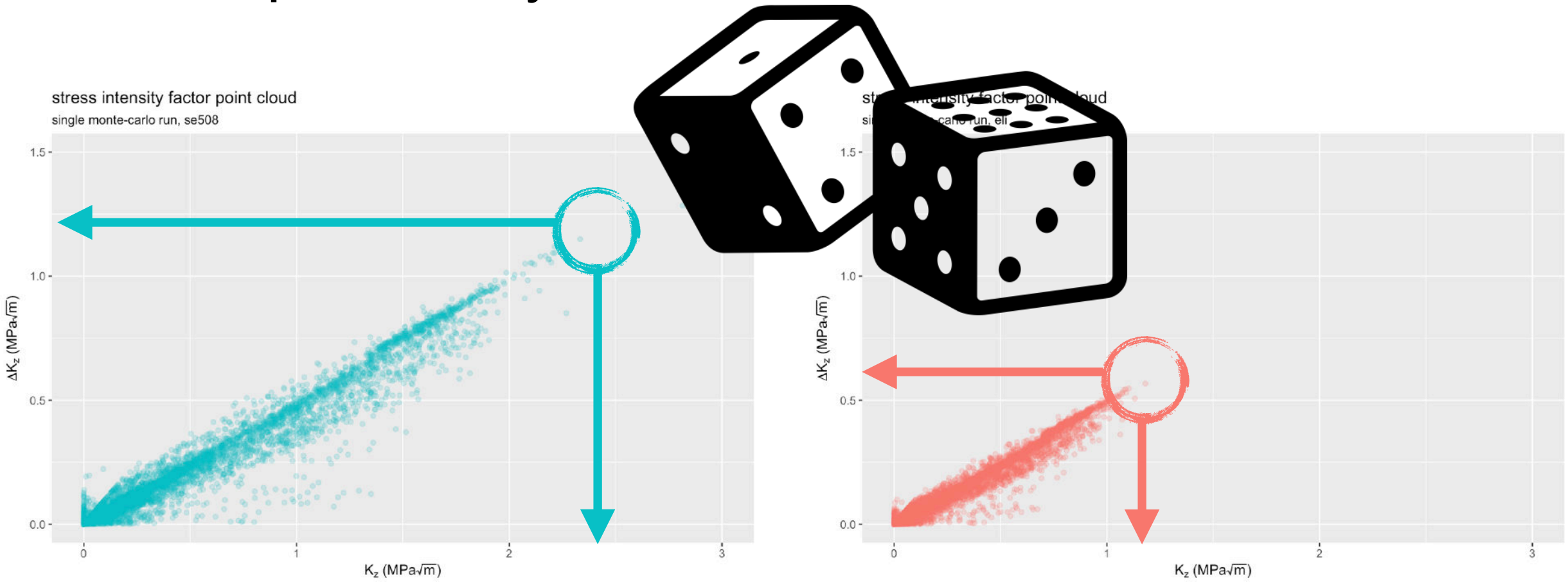

Maximum stress intensity factors for 500+500 runs

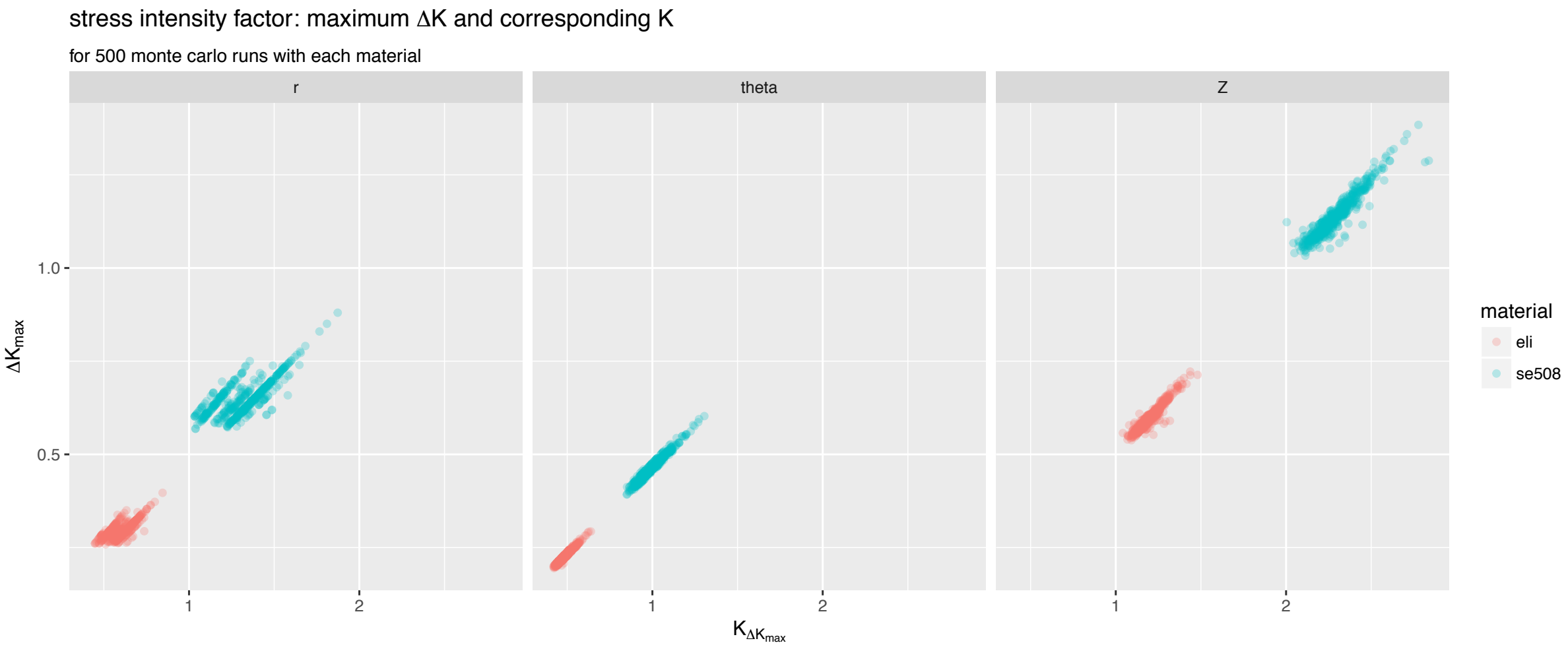

“Fortune plot” for 500+500 runs

max. ΔK_z by cyclic stress and defect (inclusion) size

unluckiest combination at upper right: largest defect at highest cyclic stress

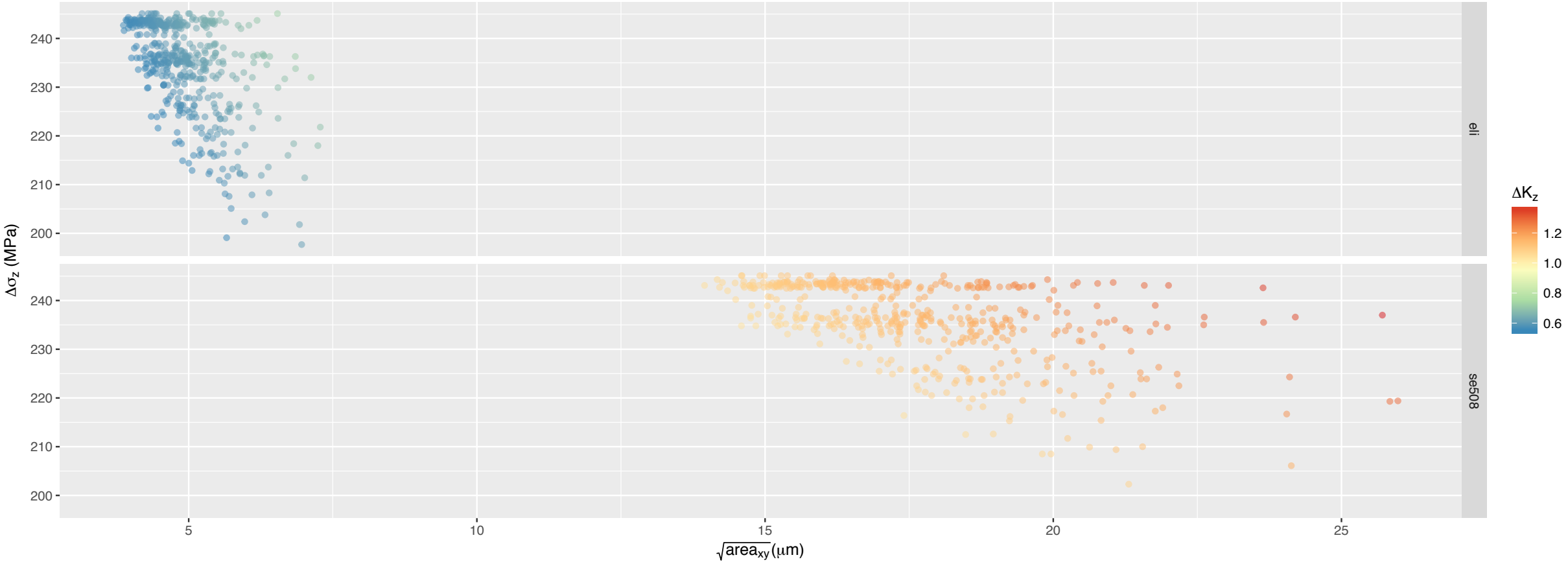

ΔK_{max} for 500+500 runs

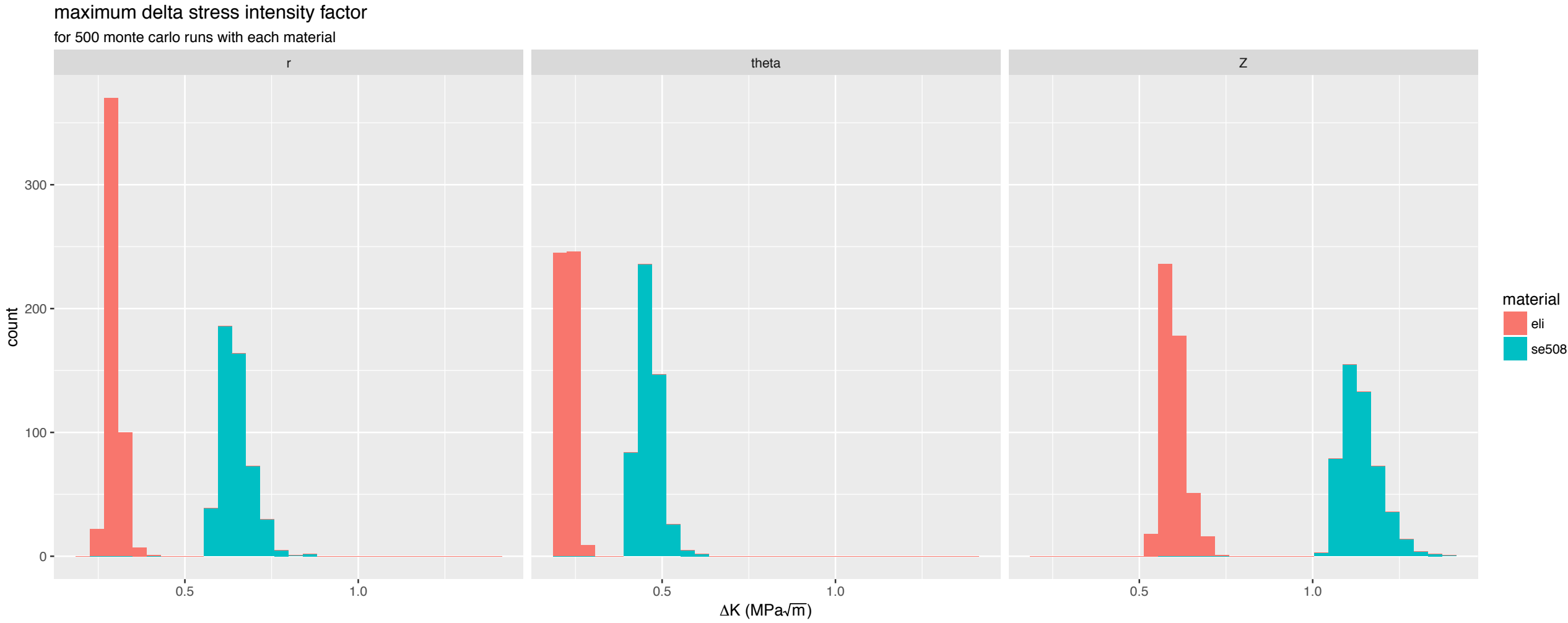

Limitations

- XCT results are currently limited to a single tubing configuration, and three sample volumes
- Resolution limit for XCT unconfirmed; comparison with conventional 2D analysis TBD
- K, ΔK are based on linear elastic fracture mechanics
- Muramaki 0.65 factor does not account for defect depth from surface
- No experimental confirmation completed (yet)
- Material properties for example FEA are unverified
- Code is all new and probably full of mistakes!

- Critical review and feedback will be greatly appreciated!

Introduction
Volumetric FEA methods
Sub-µm x-ray computed tomography
Monte-Carlo risk assessment
> **Resources**

More resources online: Nitinol Design Concepts

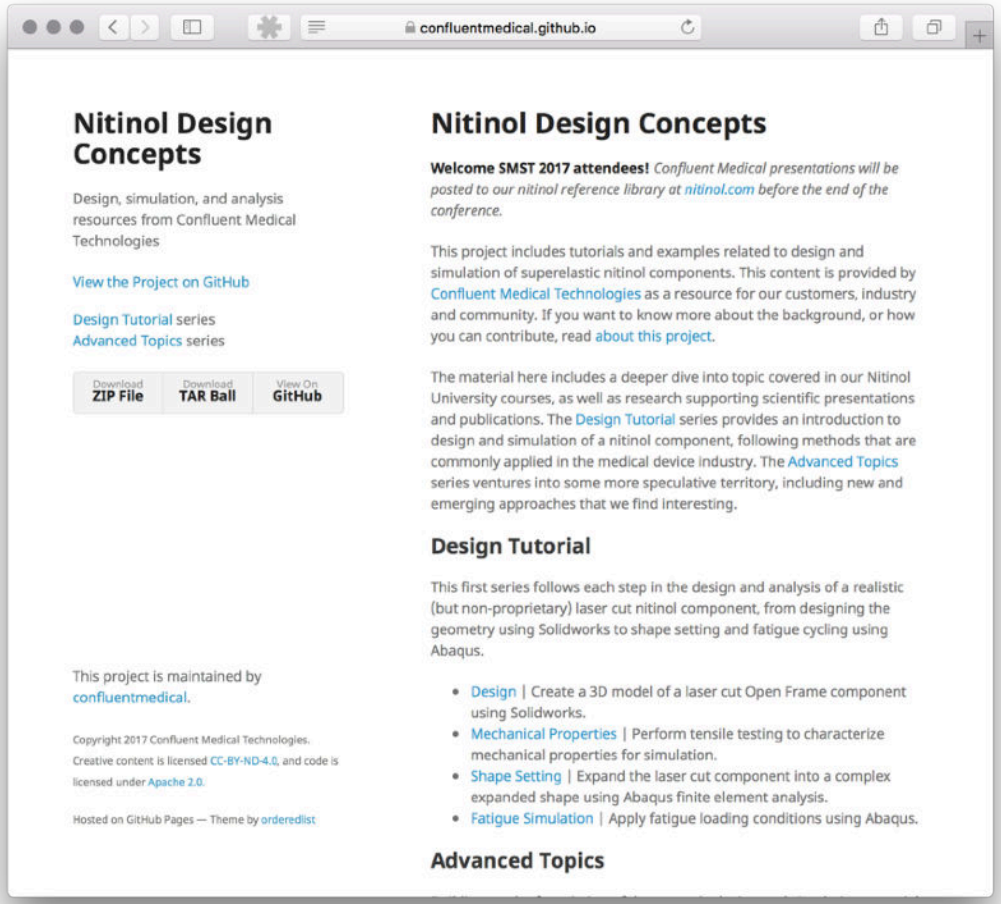

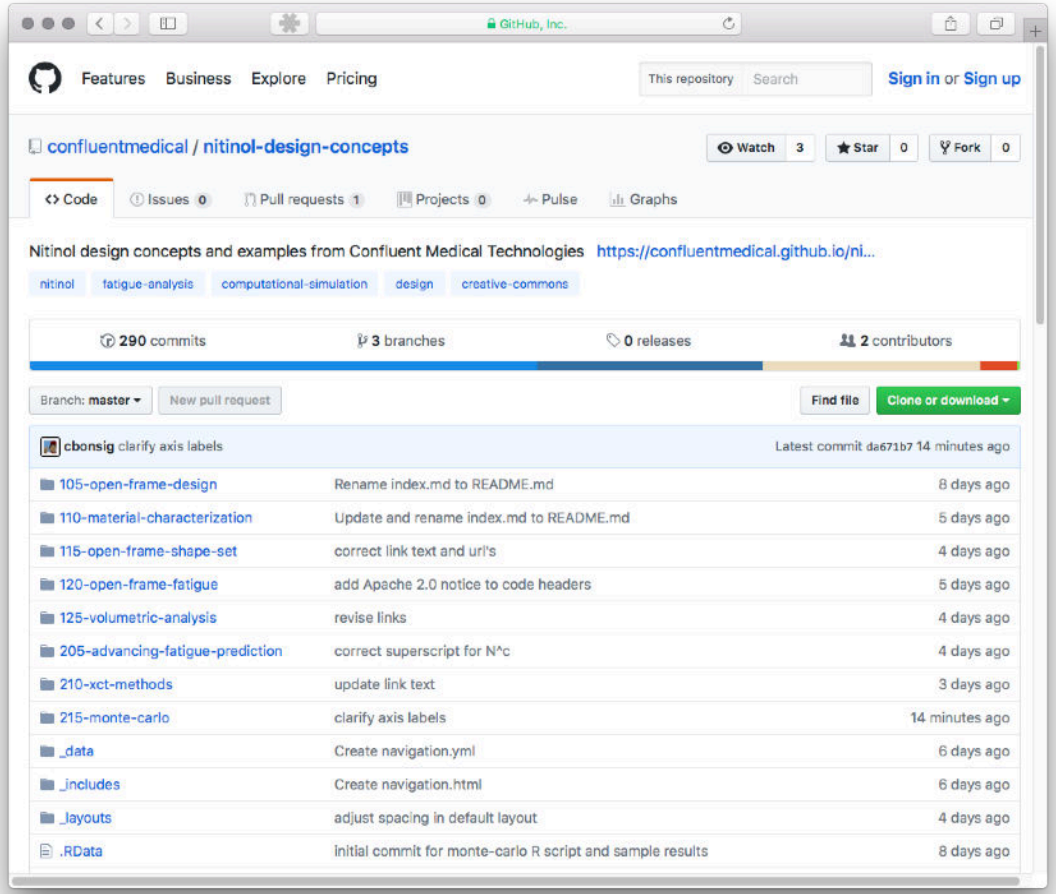

bit.ly/smst17ndc

Craig Bonsignore
Confluent Medical Technologies

craig.bonsignore@confluentmedical.com
@cbonsig